

2023

Effect of Amino Acids on the Corrosion and Metal Release from Copper and Stainless Steel

Alyssa Vander Zee
Western University

Lila Laundry-Mottiar
Western University

Saman Nikpour
Western University, snikpou3@uwo.ca

Sina Matin
Western University

Jeffrey D. Henderson
Western University

See next page for additional authors

Follow this and additional works at: <https://ir.lib.uwo.ca/chempub>

Citation of this paper:

Vander Zee, Alyssa; Laundry-Mottiar, Lila; Nikpour, Saman; Matin, Sina; Henderson, Jeffrey D.; Eduok, Ubong; Hedberg, Jonas F.; Zagidulin, Dmitriy; Biesinger, Mark C.; Noel, James J.; and Hedberg, Yolanda S., "Effect of Amino Acids on the Corrosion and Metal Release from Copper and Stainless Steel" (2023). *Chemistry Publications*. 262.
<https://ir.lib.uwo.ca/chempub/262>

Authors

Alyssa Vander Zee, Lila Laundry-Mottiar, Saman Nikpour, Sina Matin, Jeffrey D. Henderson, Ubong Eduok, Jonas F. Hedberg, Dmitrij Zagidulin, Mark C. Biesinger, James J. Noel, and Yolanda S. Hedberg

OPEN ACCESS

Effect of Amino Acids on the Corrosion and Metal Release from Copper and Stainless Steel

To cite this article: Alyssa Vander Zee *et al* 2023 *J. Electrochem. Soc.* **170** 021501

View the [article online](#) for updates and enhancements.

Investigate your battery materials under defined force!
The new PAT-Cell-Force, especially suitable for solid-state electrolytes!



- Battery test cell for force adjustment and measurement, 0 to 1500 Newton (0-5.9 MPa at 18mm electrode diameter)
- Additional monitoring of gas pressure and temperature

www.el-cell.com +49 (0) 40 79012 737 sales@el-cell.com

EL-CELL[®]
electrochemical test equipment





Effect of Amino Acids on the Corrosion and Metal Release from Copper and Stainless Steel

Alyssa Vander Zee,¹ Lila Laundry-Mottiar,^{1,a} Saman Nikpour,^{1,**} Sina Matin,^{1,**} Jeffrey D. Henderson,² Ubong Eduok,¹ Jonas F. Hedberg,² Dmitrij Zagidulin,¹ Mark C. Biesinger,^{1,2} James J. Noël,^{1,2,***} and Yolanda S. Hedberg^{1,2,3,*}

¹Department of Chemistry, The University of Western Ontario, London, Ontario, N6A 5B7, Canada

²Surface Science Western, The University of Western Ontario, London, Ontario, N6G 0J3, Canada

³Lawson Health Research Institute, London, Ontario, N6C 2R5, Canada

Copper (Cu) and stainless steel 316 L are widely used for biomedical applications, such as intrauterine devices and orthopedic/dental implants. Amino acids are abundantly present in biological environments. We investigated the influence of select amino acids on the corrosion of Cu under naturally aerated and deaerated conditions using a phosphate-free buffer. Amino acids increased the corrosion of Cu under both aeration conditions at pH 7.4. Cu release was also significantly (up to 18-fold) increased in the presence of amino acids, investigated at pH 7.4 and 37 °C for 24 h under naturally aerated conditions. Speciation modelling predicted a generally increased solubility of Cu in the presence of amino acids at pH 7.4. 316 L, investigated for metal release under similar conditions for comparison, released about 1,000-fold lower amounts of metals than did Cu and remained passive with no change in surface oxide composition or thickness. However, amino acids also increased the chromium release (up to 52-fold), significantly for lysine, and the iron release for cysteine, while nickel and molybdenum release remained unaffected. This was not predicted by solution speciation modelling. The surface analysis confirmed the adsorption of amino acids on 316 L and, to a lower extent, Cu coupons.

© 2023 The Author(s). Published on behalf of The Electrochemical Society by IOP Publishing Limited. This is an open access article distributed under the terms of the Creative Commons Attribution 4.0 License (CC BY, <http://creativecommons.org/licenses/by/4.0/>), which permits unrestricted reuse of the work in any medium, provided the original work is properly cited. [DOI: 10.1149/1945-7111/acb61c]



Manuscript submitted November 2, 2022; revised manuscript received January 23, 2023. Published February 3, 2023. *This paper is part of the JES Focus Issue on Critical Factors in Localized Corrosion in Honor of Gerald Frankel.*

Supplementary material for this article is available [online](#)

Copper (Cu) metal can be used for antimicrobial purposes (as a coating) and in intrauterine devices (for contraceptive applications) in the human body.^{1,2} For these purposes, the toxicity of Cu ions, which are released from the Cu metal through corrosion processes, is utilized towards cell membranes of bacteria or spermatozoa.¹ These Cu ions can depolarize the cell membranes of bacteria or generate reactive oxygen species.¹ The latter can also be generated through the corrosion process,³ which is a contributing factor to why Cu metal nanoparticles are more toxic than corresponding amounts of Cu ions.⁴ However, excessively high concentrations of Cu ions can cause adverse health effects, such as neurodegenerative diseases.^{5–8}

There are few studies on the effects of amino acids on Cu corrosion at physiologically relevant pH (at neutral or weakly alkaline pH), even though the ligand-induced dissolution of Cu oxide nanoparticles,⁹ Cu-containing nanoparticles,⁴ and Cu-containing minerals (weathering)¹⁰ have been known for decades. Most corrosion studies in the presence of amino acids have focused on their inhibitory effect under strongly acidic conditions,^{11–16} which are not relevant for many biological environments, including the human body.

Acceleration of the corrosion and metal release for stainless steels by organic ligands at neutral pH, but not at acidic pH, has been shown previously for citrate species,^{17–19} several other organic ligands,^{18,20} amino acids,²¹ and proteins.^{22–26}

While corrosion and ligand-induced dissolution mechanisms are related to chemical equilibrium constants and electrochemical potentials, for which data might be available for predictions, it is unclear how solution complexation relates to surface complexation. Solution complexation is, among others, related to coordination chemistry and the metal ion radius and charge.²⁷ The formation and detachment of surface complexes depend on (1) adsorption kinetics

and its influencing factors such as ionic strength, agitation, interfacial tension, and adsorbate (molecule that binds to a surface) concentration,^{28–31} (2) the crystallinity, defect density, and composition of the surface oxide,^{28,32} and (3) the presence of other species, such as other complexing agents, protons, or oxidative/reducing agents,^{28,33,34} that could assist in the surface complex detachment process.

This study aims at (1) investigating whether select amino acids influence the corrosion and metal release from Cu under physiologically relevant (pH 7.4) and phosphate-free conditions, (2) comparing the trends to stainless steel 316 L under similar experimental conditions, and (3) comparing the experimental results with equilibrium chemical speciation modelling in solution.

Experimental

Materials.—Cylindrical specimens of phosphorus-doped, oxygen-free Cu, supplied by the Swedish Nuclear Fuel and Waste Management Company (SKB) of two different batches (denoted Cu-1 and Cu-2), were used for electrochemical measurements. According to the chemical composition analysis provided by the supplier, these specimens contained >99.99% Cu and 2–3 ppm phosphorus. To ensure the electrical contact between the potentiostat and the electrode during the measurement, a stainless steel wire was spot-welded on the back of the Cu electrode. Subsequently, the electrode was embedded in epoxy resin (EpoFix, Struers) to ensure that only one face of the Cu electrode, with a known surface area, was exposed to the electrolyte during the electrochemical measurements.

A 99.9% (based on supplier information) Cu sheet (denoted Cu-3) with 0.5 mm thickness was purchased from Home Depot in London, Canada. The sheet was cut into approximately 15 × 15 mm coupons for the metal release measurements. For comparative reasons, the Cu-2 electrodes were also measured for metal release.

Stainless steel of grade S31603 (Unified Numbering System, ASTM grade 316 L), and a thickness of 2.5 mm, was cut into

*Electrochemical Society Member.

**Electrochemistry Student Member.

***Electrochemical Society Fellow.

^aPresent address: Department of Chemistry, McGill University.

^zE-mail: yhedberg@uwo.ca

coupons of approximately 15 × 15 mm. Thyssen Krupp, Germany, manufactured the 316 L sheet. The nominal composition was 16.9 wt% chromium (Cr), 1.3 wt% manganese (Mn), 10.1 wt% nickel (Ni), 0.5 wt% copper (Cu), 2.0 wt% molybdenum (Mo), 0.05 wt% nitrogen (N), 0.02 wt% carbon (C), and 0.0006 wt% sulfur (S), based on a chemical analysis provided by Aperam, France. The latter two elements are intentionally low in this grade to increase corrosion resistance. The stainless steel was used to investigate metal release and surface compositions before and after 24 h exposure to various amino acid solutions.

Chemicals, solvents, and solutions.—Chemicals were obtained in Canada from Fisher Scientific Chemical, Fisher Scientific Bioreagents, Acros Organics, Sigma Aldrich, or Millipore Sigma. The electrolytes or exposure solutions for the various investigations were composed of 9 g l⁻¹ (0.154 M) NaCl (p.a. grade), 5 mM 2-(N-morpholino)ethanesulfonic acid (MES) (low moisture content, ≥99% by titration) as a buffer, and adjusted to pH 7.3–7.4 with 8 M NaOH, 5 wt% HCl, or 2–10 wt% HNO₃. Ultrapure water (resistivity of 18.2 MΩcm, MilliporeSigma) was the solvent for all solutions. The pH adjustment was conducted for the final solution, containing all components. 9 g l⁻¹ NaCl was chosen due to its physiological relevance (0.9 wt% saline). The MES buffer was chosen because it has been reported to have minimal binding to Cu among all possible buffers.³⁵ In addition, either 0, 1, or 10 mM of amino acids were added: L-aspartic acid (98.5%), L-tyrosine (99%), L-cysteine (>98%), L-histidine (98.5%), L-arginine (>98%), L-lysine (>98%), L-threonine (>98%), glycine (≥99%), L(+)-glutamic acid (99%), L-tryptophan (99%), and L-serine (99%). Four solutions containing two different amino acids were also prepared at an equimolar concentration (0.5 mM) of each amino acid component. Amino acids were pre-selected based on chemical equilibrium modelling using the Joint Expert Speciation System (JESS);^{36,37} see below. The concentration of 1 mM total amino acid was chosen based on relevant blood plasma concentrations.³⁸ The amino acids expected to be involved in Cu complexes, based on these JESS models, were chosen for use with the Cu specimens, and those involved in Fe, Cr, and Ni complexes for the stainless steel specimens. Solutions without amino acids are denoted reference solutions. Solutions were freshly prepared or stored at 4 °C for up to 72 h and adjusted to room temperature prior to any experiment. After storage, the pH was re-adjusted, if necessary.

Cleaning procedure for glassware and contact materials.—Each glassware, plastic container, vial, or tube was acid washed and dried before use. The acid washing procedure consisted of fully submerging the container in 10 wt% HNO₃ for a minimum of 24 h, then rinsing it four times with ultrapure water, followed by air drying.

Any equipment in contact with amino acids was washed with detergent (ultra-Palmolive antibacterial hand soap) immediately after use, rinsed four times with de-ionized water, and left to dry in a fume hood before the acid cleaning. Reference electrodes in contact with amino acids were cleaned by immersion in 16 mM sodium dodecyl sulfate (Sigma Aldrich, Canada) at 40 °C for 1 h and then rinsed with ultrapure water.

Surface preparation.—*Electrochemical investigations under naturally aerated (non-deaerated) conditions.*—The Cu electrodes (Cu-1 and Cu-2) were ground successively with P300, P600, and P1200 grit SiC paper using de-ionized water as a lubricant. The electrodes were then cleaned ultrasonically in acetone and ethanol for 5 min each and dried in a flow of nitrogen gas at room temperature. The prepared electrodes were placed in an air-containing desiccator (<10% relative humidity) for 24 ± 1 h at room temperature to ensure a controlled oxide growth under controlled humidity conditions. The six different electrodes had a surface area

of 0.75–0.80 cm² (diameter of approximately 1 cm). After the oxide growth period, the Cu electrode was immersed in the naturally aerated electrolyte.

Electrochemical investigations under deaerated conditions.—The Cu electrodes were ground, cleaned, and dried as above. They were then directly immersed in a solution containing 9 g l⁻¹ NaCl and 5 mM MES buffer at pH 7.4, deaerated by sparging with ultrahigh purity argon. Upon immersion of the Cu electrode, any previously formed surface oxide was partially reduced by applying –0.8 V vs reference electrode (see below) for 30 min. The Cu electrode was then lifted out of, and above, the electrolyte while keeping it under an argon atmosphere. Then, an amino acid solution (50 ml of freshly prepared stock solution in ultrapure water) was added to 450 ml of the non-replenished electrolyte. The late amino acid addition ensured that the amino acid was not affected by the electrochemical reduction procedure of Cu. Then, the electrode was immersed back into the electrolyte and sparged with argon. The argon flow rate decreased after 15 min of sparging and continued during the remaining electrochemical measurement.

Metal release from Cu.—For comparative reasons, the Cu coupons (Cu-3) and the Cu electrode (Cu-2) were ground, cleaned, dried, and stored in a desiccator as described for the naturally aerated conditions above. The surface area of each coupon or electrode was measured individually.

Metal release and surface analysis of stainless steel coupons.—The stainless steel coupons were polished with P1200 grit SiC paper using water as a lubricant, cleaned by sonicating for 5 min in acetone followed by 5 min in ethanol, dried with nitrogen gas at room temperature, and stored in a desiccator (24 ± 1 h) at <10% relative humidity and room temperature. The edges of the stainless steel coupons were sealed with a clear lacquer (acrylate nail polish) before storage in the desiccator to avoid any preferential corrosion at the edges of a material that might be susceptible to localized corrosion.

Electrochemical measurements.—For the electrochemical measurements, the Cu electrode served as the working electrode and a platinum wire as the counter electrode. For the reference electrode, either Ag/AgCl, KCl (3 M) or Ag/AgCl, KCl (sat.) was used. They were both checked against a master reference electrode (saturated calomel reference electrode) before each experiment. Unless otherwise specified, all potentials are presented vs Ag/AgCl KCl (sat.).

The open circuit potential was recorded for 1 h prior to the potentiodynamic polarization. Forward (positive-going) and reverse (negative-going) scans at 1 mV s⁻¹ were performed, starting at –0.2 V vs the previously measured open circuit potential and ending at either 1.2 V vs reference electrode (Ag/AgCl, KCl (3 M or saturated)) or when the current was greater than 0.5 mA. The forward scan was followed by the reverse scan ending either at the previously measured open circuit potential or when the current became cathodic. To extract the corrosion current density (*i*_{corr}) and corrosion potential (*E*_{corr}) from the potentiodynamic polarization curves, Tafel analyses were performed using VersaStudio (version 2.61.3, Princeton Applied Research). All conditions were tested in at least two replicate measurements.

Metal release test procedure and analysis.—*Procedure.*—Triplicates of specimens (Cu-3 and 316 L) and one blank (background control of a solution without Cu or stainless steel coupons) were tested in each solution. Triplicates of Cu-2 electrodes and a blank solution were tested in the reference solution (no amino acids) for comparison. A 1 cm²/ml surface area to solution volume ratio was maintained in all cases. The chosen containers/vials ensured that both coupon faces were exposed to the solution. The pH of the solution was measured prior to the metal release test procedure in the prepared solution and afterwards individually in each vial. After the

solution was added to the vials containing the coupons, or no coupon in the case of the blank samples, they were placed in an Incubating Rocking Platform Shaker, which had been set to a temperature of 37 ± 0.5 °C. They were incubated for 24 h with bilinear agitation (10° tilt with 22 ± 1 cycles/min). After 24 h, the specimens were removed from the solutions with acid-cleaned (1 wt% HNO₃) tweezers. The surfaces were rinsed with 1 ml of ultrapure water (for Cu) or 1 ml of extra blank reference (no amino acid) solution (for stainless steel coupons), which was added to the metal release solution. This procedure ensured the solution sampling of any loosely surface-adhered species and cleaned the surface for future surface analysis. After the rinsing step, the coupons were dried with a flow of nitrogen gas at room temperature, placed separately in a closed plastic container, and stored in a vacuum desiccator before any surface analysis. After exposure to stainless steel coupons, the solution samples were acid-digested by adding microvolumes of ultrapure 65 wt% HNO₃ until the pH was less than 2. They were then stored at 4 °C until the solution analysis was performed. Spiked samples containing known amounts of Fe, Cr, Ni, and Mo were also prepared for each blank amino acid solution to detect any matrix effects (deviations from nominal concentration due to effects, such as interferences or change in plasma temperature, of the solution composition).

The solution samples, after exposure to Cu specimens, were digested using a Milestone ETHOD microwave digester (170 °C, 10 min ramp, 10 min hold), at the Biotron facility (Western University), for a dilution factor of 3.33 (3 ml sample in 10 ml total volume) and an acid:sample factor of 5:45, where the acid was pure (trace metal basis) HNO₃ (>68 wt%). The digestion was modified from EPA 3015 (METHOD 3015 A). Spiked samples (with known amounts of Cu) were also prepared in parallel for quality control. The digested solution samples were stored at room temperature before solution analysis.

Analysis.—A Thermo Scientific iCAP Q inductively coupled plasma mass spectrometer with helium collision gas for Fe, Cr, Mo, and Ni, and no reaction gas for Cu, was calibrated with the six prepared standards (0, 5, 10, 20, 50, 100 $\mu\text{g l}^{-1}$) of Fe, Cr, Mo, and Ni (multi-standard) to create four linear calibration curves (Fe $R^2 = 0.9995$, Cr $R^2 = 0.9999$, Mo $R^2 = 0.9999$, Ni $R^2 = 0.9997$) or with five prepared standards (0, 30, 100, 500, and 1,000 $\mu\text{g l}^{-1}$) for Cu ($R^2 = 0.9938$ – 0.9989). The detection limits, defined as instrument detection limit plus background equivalent concentration, for Fe, Cr, Mo, Ni, and Cu were as follows: 2.5, 0.23, 0.02, 0.17, and 0.5 $\mu\text{g l}^{-1}$, respectively. The uncertainty (relative percentage deviation from expected value) for a 50 $\mu\text{g l}^{-1}$ Fe/Cr/Mo/Ni quality control standard was 0.13% for Fe, 1.58% for Cr, 2.18% for Mo, and 0.56% for Ni. The uncertainty for 10 and 50 $\mu\text{g l}^{-1}$ quality control standards was 11% and <8%, respectively.

Calculations.—An analytical balance with 0.1 mg readability was used to measure the exact masses of stock solutions and final standards or quality control samples. Due to the influence of chlorides on the plasma temperature, the chloride concentration was kept constant in all standards and samples. The final concentration of each standard or quality control sample was calculated according to Eq. 1.

$$c = \frac{m_{\text{Stock}}}{m_{\text{final}}} \times c_{\text{Stock}} \quad [1]$$

where m_{Stock} denotes the mass of the added stock solution (certified standards), m_{final} denotes the final mass of the sample, and c_{Stock} represents the concentration of the stock solution.

The dilution factor (DF) is the final volume divided by the initial sample volume. All dilution factors (from rinsing, digestion, and any additional dilutions) are multiplied to determine the initial sample concentration. The amount of metal released per unit coupon surface area ($\mu\text{g}/\text{cm}^2$) is calculated by Eq. 2.

$$\text{Released amount} = \frac{(c_{\text{sample}} \times \text{DF}_1 \times \text{DF}_2 \times \text{DF}_3 - c_{\text{blank}} \times \text{DF}_1 \times \text{DF}_2 \times \text{DF}_3) \times V_{\text{exposure}}}{A} \quad [2]$$

where c_{sample} in $\mu\text{g}/\text{l}$ denotes the concentration that was measured for a particular solution sample (in previous contact with a metal coupon), c_{blank} in $\mu\text{g}/\text{l}$ is the corresponding measured concentration of the blank sample (without any contact with a metal coupon, but otherwise identical exposure conditions), $\text{DF}_{1,\dots,3}$ (unitless) denote the individual dilution factors (1 if no dilution occurred), V_{exposure} (in L) represents the volume during the exposure (for example 5 ml for a 5 cm^2 coupon), and A (in cm^2) denotes the non-sealed surface area of the Cu or stainless steel coupon.

Average values and standard deviations of triplicate samples are shown in the following.

Surface analysis.—The X-ray photoelectron spectroscopy (XPS) analyses with an information depth of 7–10 nm and detection limits of 0.1–0.5 at% were carried out on two different locations of unexposed (for reference) and exposed stainless steel coupons or one location of Cu coupons (Cu-3). XPS was run with a Kratos AXIS Supra X-ray photoelectron spectrometer using a monochromatic Al K $_{\alpha}$ source (15 mA, 15 kV). The instrument work function was calibrated to give a binding energy (BE) of 83.96 eV for the Au 4f_{7/2} line for metallic gold. The spectrometer dispersion was adjusted to give a BE of 932.62 eV for the Cu 2p_{3/2} line of metallic copper. The Kratos charge neutralizer system was used on all specimens. All samples were mounted electrically isolated from the instrument sample holder for these analyses. Survey scan analyses were carried out with an analysis area of $300 \times 700 \mu\text{m}$ and a pass energy of 160 eV. High-resolution analyses were carried out with an analysis area of $300 \times 700 \mu\text{m}$ and a pass energy of 20 eV. For Cu coupons, the Cu 2p and Cu LMM signals were collected first before proceeding with other spectra to minimize any possible reduction of Cu^{II} species, which can occur during prolonged X-ray exposure.³⁹ Spectra have been charge-corrected to the main line of the C 1s spectrum (adventitious carbon) set to 284.8 eV. Spectra were analyzed using CasaXPS software (version 2.3.14). The spectra were fitted using the fitting parameters specified previously.^{39,40}

Chemical speciation equilibrium modelling.—The Joint Expert Speciation System (JESS, version 8.8 v)^{36,37} was used to determine the equilibrium chemical speciation in the various solutions for 1 mM of total Cu, Fe, Cr, and Ni. The solution oxidation-reduction potential input values were pe 3.4 ($E_h = 200 \text{ mV}_{\text{SHE}}$, only for Cu) and pe 5 ($E_h = 300 \text{ mV}_{\text{SHE}}$) for deaerated and naturally aerated conditions, respectively. The definition of pe is the negative logarithm of the electron activity, $\text{pe} = -\log [e^-]$, or $E_h = 2.3 \text{ RT pe}/F$, where E_h denotes the solution oxidation-reduction potential in V, with reference to the standard hydrogen electrode, R the gas constant (8.3145 CV/(mol K)), T the temperature in K, and F the Faraday's constant (96,485.3321 C mol⁻¹). Other input values were 1 mM of the respective amino acid, 9 g l⁻¹ NaCl, pH values of 5, 6.5 and 7.4, a temperature of 25 °C, and a pressure of 1 atm. The lower pH values simulate oxidative conditions present under anodic polarization,⁴¹ and the temperature was chosen to benefit from the best availability of literature data. Solids were allowed to form and precipitate. In one case, the calculations were performed for 1 mM Cu at 25 °C in all 19 natural amino acids (1 mM each), 9 g l⁻¹ NaCl, pe 5, pH 7.4, and 1 atm pressure. The equation-solving algorithm was damped Newton-Raphson with maximal iterations of 200 and a maximum delta[log(unknown)] of 2.0. The convergence criterion was either that the sum of absolute equation values was <0.04 or that each delta[log(unknown)] was <0.0001. Only successfully solved equations were considered in the following. In very few

cases, one species caused a numerical error and was, in that case, excluded, as indicated in the corresponding results. JESS uses an extensive database of reactions with verified dissociation constants and standard potentials from peer-reviewed data. In all cases, the database included reactions between the element of interest (Cu, Fe, Cr, Ni) and the reactant of interest (chlorides and at least one amino acid). The number of reactions processed ranged from 62 (reference solution for Fe) to 574 (Cu with all 19 amino acids). Details concerning the reactions for each element and solution are given in the supplementary data (online only).

Statistics.—Any statistically significant difference was determined between two sets of data using a student's t-test with unequal variance and for unpaired data because of different coupons/electrodes, using the KaleidaGraph (Synergy, v. 4.0) software. If the probability of the data being equal was less than 0.05 ($p < 0.05$), the difference was considered statistically significant.

Results and Discussion

Corrosion of copper in the presence of amino acids under naturally aerated conditions.—Figure 1 gives an overview of potentiodynamic polarization curves of Cu electrodes in 9 g l^{-1} NaCl, buffered by 5 mM MES buffer to pH 7.4, without amino acids (reference) or with 1 mM of different amino acids. For both replicates (Figs. 1a and b), the reference solution shows the highest corrosion potential and lowest corrosion current, further illustrated in Fig. S1 (supplementary data). Under naturally aerated conditions, all reverse (negative-going) scans exhibited lower currents than the forward (positive-going) scans (Fig. 1). However, considerable variability was found for the case of threonine and for different Cu materials, further discussed below. Because of the low number of replicate measurements and the observed variability, the electrochemical data are not further discussed for individual amino acid solutions. It is, however, clear that amino acids, especially some of them, were able to increase the corrosion current density (up to 10-fold: 4,300 compared with 455 nA cm^{-2}) and to decrease the corrosion potential compared to that in the reference solution at pH 7.4 under aerated conditions. The corrosion potential can shift in the

negative direction for two reasons: increased anodic reaction rate or decreased cathodic reaction rate. Both options are possible here: The slope of the cathodic branch in the presence of amino acids is equal to or smaller than it is in their absence (Fig. 1). The adsorption of amino acids has been shown to decrease the cathodic reaction rate^{13,42} and the corrosion current density^{13,42,43} in studies at lower pH, well below the lowest pK_a values of the amino acids. In those studies, the amino acids would be fully protonated and not expected to form metal complexes (further discussed below). Therefore, they would not affect the anodic half-cell reaction rate.^{13,42,43} In one study in 1 M HNO_3 , it was found that cysteine, lysine, and arginine inhibit the corrosion of Cu, but glycine and valine accelerate it slightly.⁴⁴ In our study at pH 7.4, the higher corrosion current density in the presence of the amino acids and the higher release of Cu into the solution (see below) suggest that all amino acids tested increase the anodic reaction rate.

Corrosion of copper in the presence of amino acids under deaerated conditions.—The human body and many other environments can have varying concentrations of oxygen and other oxidative or reducing species. To investigate whether dissolved oxygen influences any amino acid-induced acceleration of Cu corrosion, electrochemical measurements were also conducted under deaerated conditions on Cu electrodes that were partially reduced electrochemically before adding amino acids. Oxygen-free environments are relevant in certain parts of the human body and closed environments after oxygen has been consumed.

Figure 2 depicts a comparison of the behavior of Cu in 9 g l^{-1} NaCl at pH 7.4 under naturally aerated and deaerated conditions in the absence of amino acids (a), and the presence of 1 mM serine (b), 1 mM threonine (c), and 1 mM tyrosine (d). These three amino acids were selected based on their strong corrosion-accelerating properties under naturally aerated conditions. In all solutions, the corrosion potential was lower under deaerated conditions than naturally aerated conditions. However, the difference was small in the presence of tyrosine. The slope of the anodic branch was steeper (higher rate) under naturally aerated conditions than under deaerated conditions in all cases, Fig. 2, which is related to the presence of the dominant oxidant,

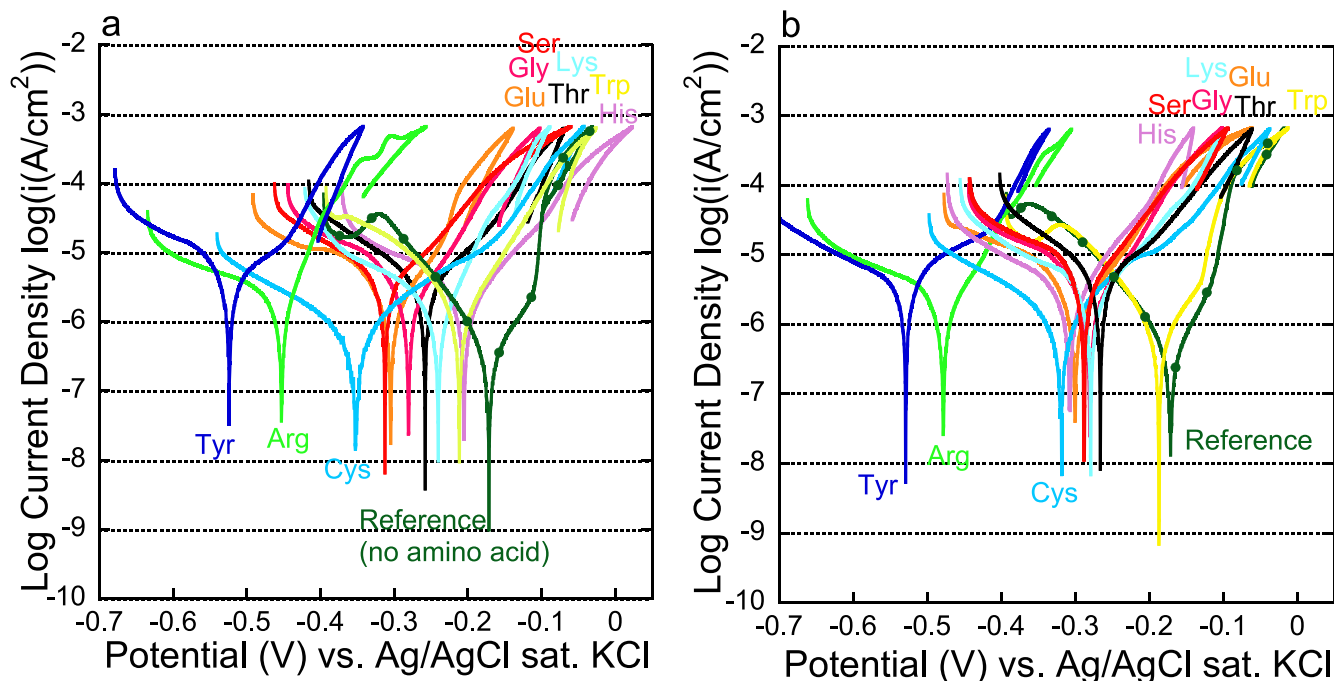


Figure 1. Potentiodynamic polarization curves for two replicates of Cu specimens (Cu-1) exposed to various naturally aerated amino acid solutions. All Cu specimens were polished and desiccated for 24 h before immersion in the solutions of 9 g l^{-1} NaCl, 5 mM MES buffer, and 1 mM of various amino acids at pH 7.40 and 25 °C. (a) replicate 1, and (b) replicate 2. The corresponding corrosion potential and corrosion current density are shown in Fig. S1, supplementary data.

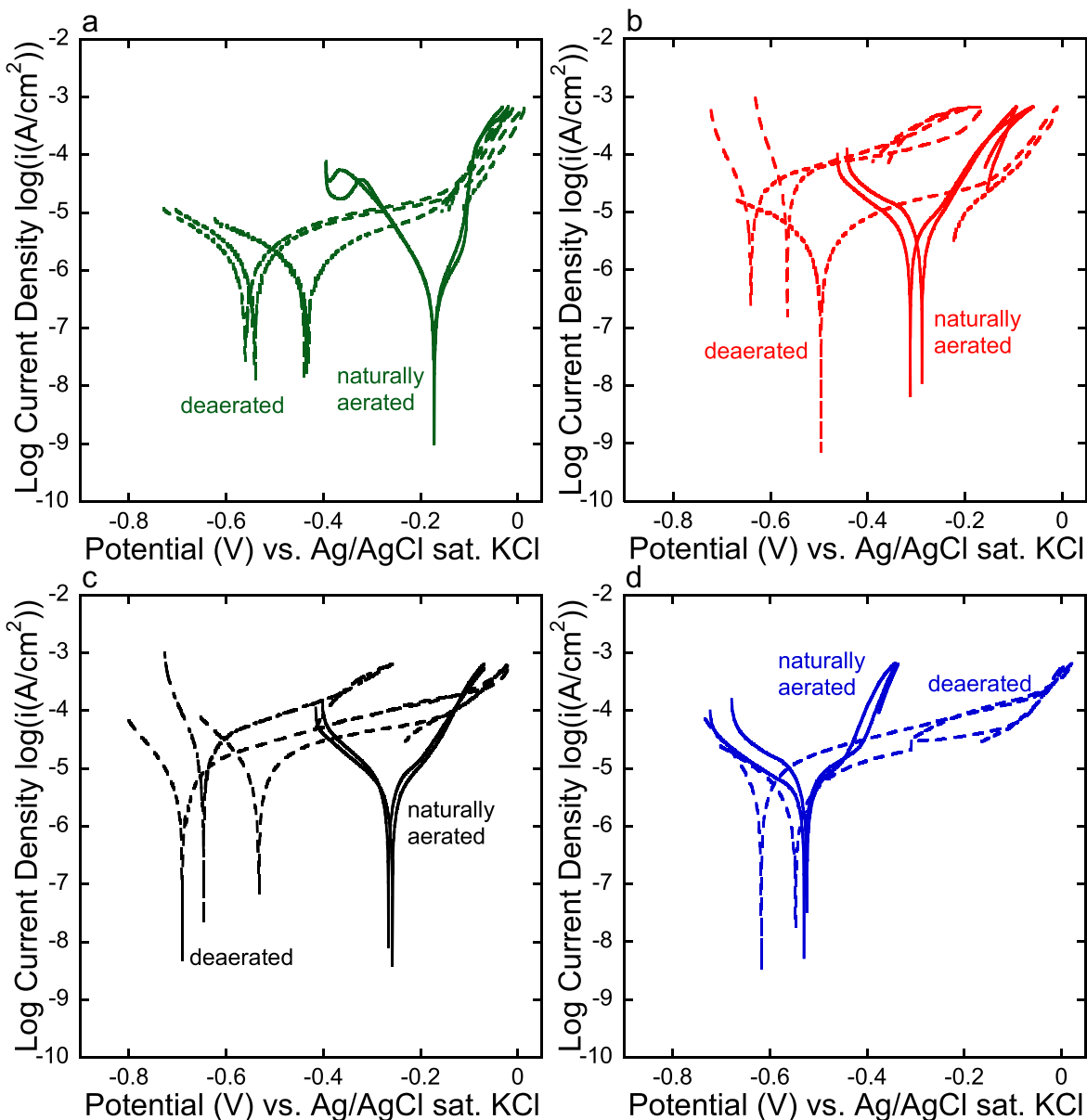


Figure 2. Comparison of potentiodynamic polarization curves in deaerated and naturally aerated solutions (Cu-1). Potentiodynamic polarization under deaerated (dashed lines in a–d) or aerated (solid lines in a–d) conditions in 9 g l^{-1} NaCl, 5 mM MES buffer, at pH 7.40 and $25 \text{ }^\circ\text{C}$ (a), or with the addition of 1 mM of serine (b), threonine (c), or tyrosine (d). For deaerated conditions, the Cu specimens were freshly polished and electrochemically reduced, and the electrolyte was deaerated. For naturally aerated conditions, the Cu specimens were polished, stored in a desiccator for 24 h, and then immersed in a non-purged electrolyte.

oxygen, under naturally aerated conditions. In contrast to scans recorded under naturally aerated conditions (Fig. 1), the backwards scan in the presence of serine (Fig. 2b) and tyrosine (Fig. 2d) under deaerated conditions displayed slight positive hysteresis. The corrosion current density was 2.7-fold higher under deaerated conditions than under naturally aerated conditions for the reference solution (no amino acids). This is likely related to the freshly polished and reduced surface, compared with a surface that had been allowed to form a surface oxide for one day. Likewise, the corrosion current density was higher under deaerated conditions than under naturally aerated conditions (about 3-fold) in the presence of serine and threonine, but not tyrosine. The corrosion current density was up to 11-fold higher in the presence than in the absence of amino acids under deaerated conditions ($14 \mu\text{A cm}^{-2}$ compared with $1.2 \mu\text{A cm}^{-2}$). However, there was considerable variability among the replicate measurements under deaerated conditions, as further discussed below.

Variability and uncertainties in electrochemical measurements.—Figure A-1 (Appendix) shows the variability among replicate measurements made in aerated and deaerated solutions containing threonine. One of the replicate measurements for the Cu-1 electrode in 1 mM threonine under aerated conditions showed a very different electrochemical behavior than all other measurements in this study, indicating localized corrosion (positive hysteresis during the backwards scan), Fig. A-1. Therefore, further replicate measurements were conducted with a different batch (Cu-2) since the Cu-1 electrodes were not available anymore. These two measurements showed similar or lower corrosion current density and behavior (no localized corrosion behavior) to that displayed during the first two replicate measurements with Cu-1. We also tested threonine at a higher concentration (10 mM) under naturally aerated conditions, Fig. A-1, which did not indicate any localized corrosion behavior. Under deaerated conditions, however, the two batches of Cu electrodes (Cu-1 and Cu-2) differed considerably, Fig. A-1, with significantly lower corrosion current density for Cu-2 than for Cu-1.

A similar trend was found in deaerated 1 mM serine solution, Fig. S2 (supplementary data).

Considering these variabilities and uncertainties, the electrochemical data will only be discussed qualitatively in the following.

Solution speciation modelling of Cu.—Equilibrium chemical speciation data are not necessarily comparable to a kinetic process, as investigated by the electrochemical and metal release studies. Kinetics are influenced by many factors, including the time-limiting detachment process of surface complexes,³³ oxide thickness and properties, and mass transport of oxidants and ions from/to the surface.⁴⁵

Figure 3 shows a simplified overview of results from equilibrium speciation modelling for the reference solution (9 g l^{-1} NaCl) without and with 1 mM of serine, threonine, and tyrosine, as well as 19 amino acids (1 mM each), for a total Cu concentration of 1 mM. The different aeration conditions were simulated with input values of a pe of 5 (naturally aerated) and a pe of 3.4 (deaerated). In the reference solution at pH 7.4 (Fig. 3a), Cu was predicted to be entirely or primarily solid (CuO at pe 5 and Cu_2O at pe 3.4). When the pH decreased to pH 6.5 and 5, as expected for the surface pH of the electrode during anodic polarization,⁴¹ the relative concentration of aqueous Cu-chloride species increased. There were no solid species predicted at pH 5. The fraction of aqueous species increased strongly compared with that of the reference solution in the presence of 1 mM serine (Fig. 3b). The dominant solid species at pH 7.4 was predicted to change from CuO (54% of total Cu) to Cu_2O (59% of total Cu) when pe was changed from 5 to 3.4. The remaining

aqueous species at pH 7.4 were entirely Cu^{II} -serine complexes at pe 5, and Cu^{II} -serine complexes and CuCl_2^- at pe 3.4. When the pH decreased, the fraction of aqueous Cu-serine complexes decreased (50% at pH 6.5 and pe 5, 21% at pH 6.5 and pe 3.4, 24% at pH 5 and pe 5, and 1% at pH 5 and pe 3.4) and the fraction of aqueous Cu-chloride species increased (Fig. 3b). At pH 6.5, 46 and 60% of the total Cu were predicted to be solid at pe 5 and 3.4, respectively. At pH 5, there were no solid Cu species among the five predominant species. Figure 3c shows the five predominant species for the solution containing threonine. At pH 7.4, the prevalence of aqueous threonine species decreased slightly with deaeration (from 70% of total Cu to 58% of total Cu). At lower pH, chloride complexes took over. At pH 5, no solid species were predicted. A similar trend was predicted for tyrosine, Fig. 3d, with 46 and 42% aqueous tyrosine species predicted at pH 7.4 under naturally aerated and deaerated conditions, respectively. When all 19 amino acids were present, no solid species or Cu-chloride species were predicted at any pH or aeration condition, Fig. 3e. A larger fraction of Cu^{I} complexes formed with amino acids under deaerated than aerated conditions. A wide variety of mainly multidentate (involving various amino acids) complexes was predicted to form in the solution with 19 amino acids.

These speciation model results confirm the experimental observation that amino acids can increase the solubility of Cu ions under both naturally aerated and deaerated conditions.

Copper release and chemical speciation modelling under naturally aerated conditions.—The released amount of Cu was

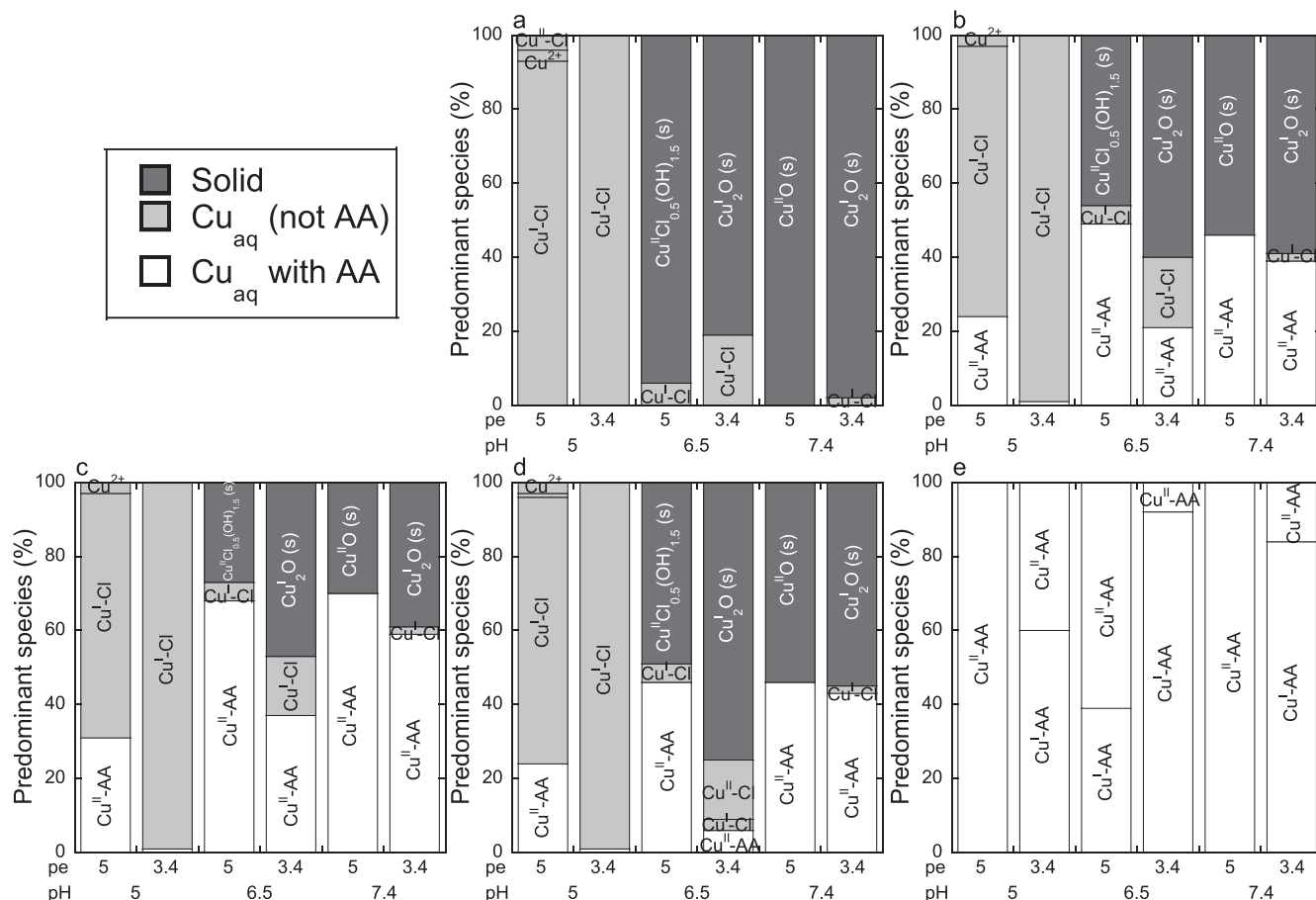


Figure 3. Predominant Cu species in different solutions, modelled by JESS. 9 g l^{-1} NaCl, $25 \text{ }^\circ\text{C}$, and 1 atm pressure, with no additional amino acids (a), 1 mM serine (b), 1 mM threonine (c), 1 mM tyrosine (d), and 1 mM each, of arginine, asparagine, aspartic acid, cysteine, glutamic acid, glutamine, glycine, histidine, isoleucine, leucine, lysine, methionine, phenylalanine, proline, serine, threonine, tryptophan, tyrosine, and valine (e). The pe was varied from pe 5 ($E_h = 300 \text{ mV}_{\text{SHE}}$) to pe 3.4 ($E_h = 200 \text{ mV}_{\text{SHE}}$), and the pH was 7.4, 6.5, and 5. Values are given in % (of 1 mM total Cu), and the valence state is indicated for all aqueous species. Further details are provided in tables S1-S5 (supplementary data). Abbreviations: s—solid; aq—aqueous; AA—amino acid.

determined in solution after one day of immersion of Cu coupons (Cu-3) in the various solutions at 37 °C (body temperature) under naturally aerated conditions (Fig. 4). The Cu release was higher (statistically significant) in all 10 different amino acid solutions than in the reference solution without any amino acid. The greatest absolute differences, 18, 11, and 10-fold, were observed for cysteine, lysine, and tyrosine, respectively, and the greatest statistical significance of the difference was seen for histidine. The lowest differences were found for serine (1.4-fold increase) and threonine (2-fold).

For comparison, the Cu electrode material Cu-2 was also measured in the reference solution (no amino acids) and showed a slightly lower (not statistically significant) release ($7.3 \mu\text{g cm}^{-2}$ compared with $13 \mu\text{g cm}^{-2}$), Table A.1.

Table A.11 shows the fraction of predicted aqueous species based on equilibrium modelling at pH 7.4 and p_e 5. It supports the higher solubility of Cu in amino acid solutions than in the reference solution. However, it predicted histidine and cysteine to result in the largest solubility, which only partially correlated with the experimental data (cysteine resulted in the highest release). A direct comparison might be difficult, as the equilibrium data does not consider kinetics and assumes the pH to be constant at pH 7.4.

Figure A.2 shows the actual pH data during 24 h of exposure. All amino acids induced some pH change during the 24 h exposure. Serine, glycine, cysteine, arginine, and tyrosine decreased the pH to values between pH 6 and 7, which according to the chemical speciation modelling (Fig. 3) results in an increased predicted solubility. The corrosion reaction of Cu increased in some cases the pH, resulting in higher final pH values than in the corresponding blank solution without a Cu coupon. This indicates the generation of hydroxyl anions during the cathodic reaction (Eq. 3).

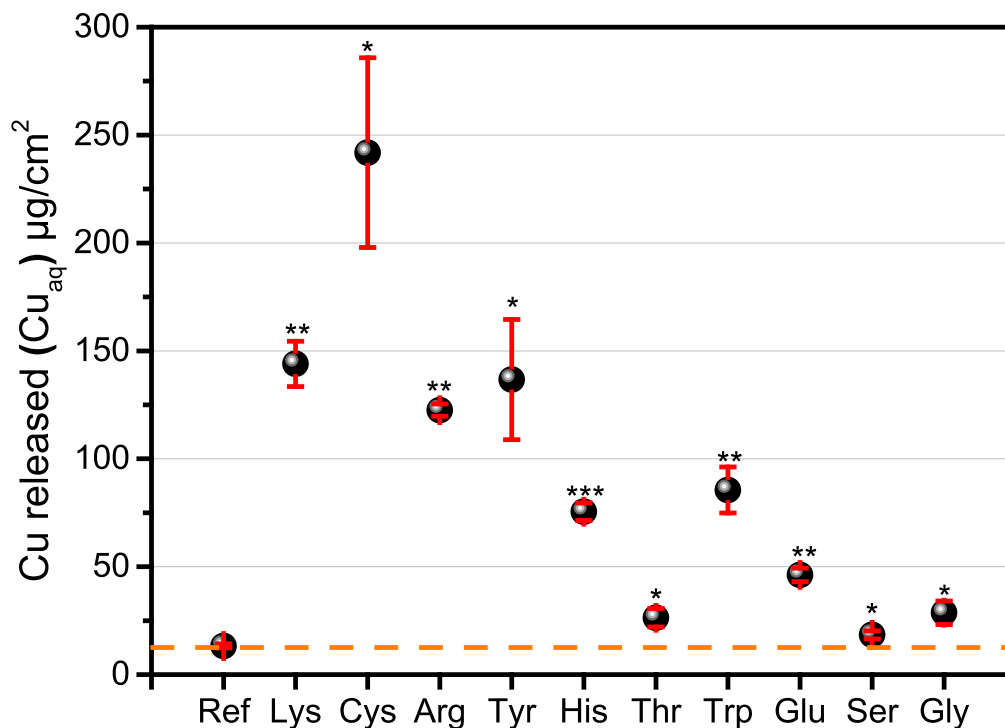


Figure 4. Amounts of Cu released from Cu coupons (Cu-3) in various solutions. Determined aqueous (released) Cu after 24 h exposure of Cu coupons at 37 ± 0.5 °C in naturally aerated 9 g l^{-1} NaCl, 5 mM MES buffer, pH 7.4, containing no amino acid (Ref), or 1 mM tyrosine (Tyr), arginine (Arg), tryptophan (Trp), cysteine (Cys), histidine (His), glutamic acid (Glu), lysine (Lys), serine (Ser), threonine (Thr), or glycine (Gly). The error bars show the standard deviation of triplicate samples, except for Arg, which only had duplicate samples. The dashed line indicates the value for the Ref solution. Any statistically significant differences compared with the Ref solution are shown by asterisks (* - $p < 0.05$; ** - $p < 0.01$, *** - $p < 0.001$). The corresponding values are shown in Table A.1.

Table I. Average and standard deviation of the ratio between the sum of the C2, C3, and C4 peak areas to the total C 1s peak area for stainless steel 316 L and Cu coupons exposed to 9 g l^{-1} NaCl and 5 mM MES buffer at pH 7.4 and 37 °C for 24 h with and without 1 mM of respective amino acids (as indicated). A reference coupon before exposure is also measured. Duplicate measurements were conducted for 316 L and a single measurement for Cu. Asterisks indicate statistically significant differences to the reference solution (* - $p < 0.05$, ** = $p < 0.01$).

Solution/Sample	316 L (C2+C3+C4)/C _{total}	Cu
Unexposed coupon	0.19 ± 0.07	Not analyzed
Reference solution	0.22 ± 0.01	0.19
Lysine	0.35 ± 0.05	Not analyzed
Cysteine	$0.35 \pm 0.01^{**}$	Not analyzed
Arginine	$0.37 \pm 0.01^{**}$	Not analyzed
Tyrosine	0.37 ± 0.06	0.24
Histidine	$0.31 \pm 0.01^*$	Not analyzed
Threonine	0.38 ± 0.11	0.26
Serine	Not analyzed	0.32
Aspartic acid	0.35 ± 0.03	Not analyzed

Amino acids can affect Cu corrosion and Cu release in several ways. First, they can shift the equilibrium of the anodic reaction (Cu oxidation to Cu^{2+}) towards dissolution by complexing released Cu ions. Second, amino acids can form surface complexes and cause ligand-induced dissolution. This is believed to be the dominant mechanism at neutral pH for Cu oxides.^{9,10,46} Third, by assisting the dissolution of the surface oxide, the amino acids can indirectly influence Cu metal oxidation driven by the cathodic reaction (dependent on available oxygen). Fourth, they can change the local surface pH through adsorption by attracting counter-ions such as

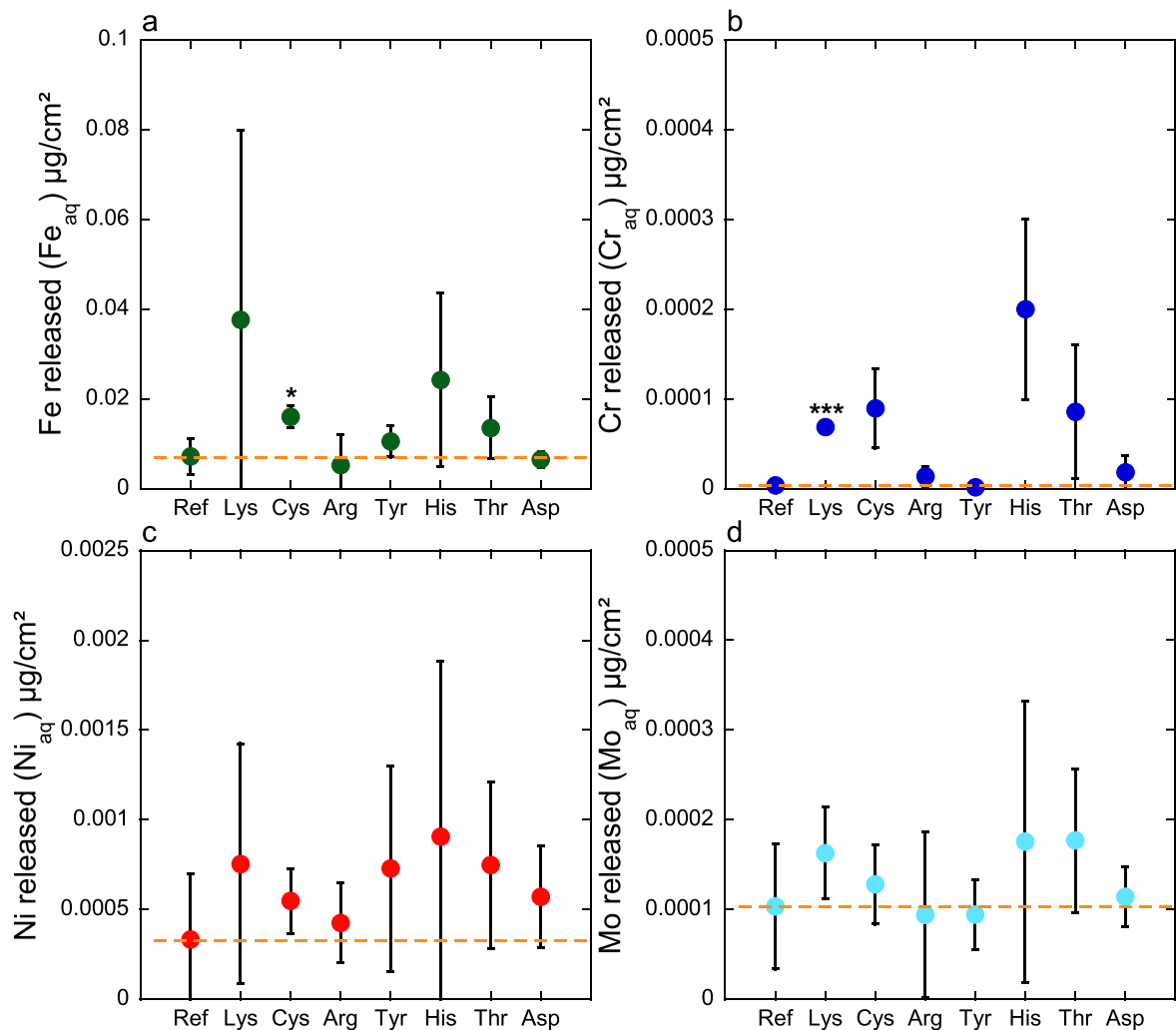


Figure 5. Amounts of metals released from stainless steel coupons in various solutions. Determined aqueous (released) Fe (a), Cr (b), Ni (c), and Mo (d) after 24 h under naturally aerated exposure of stainless steel 316 L coupons at 37 ± 0.5 °C in 9 g l^{-1} NaCl, 5 mM MES buffer, pH 7.4, containing no amino acid (Ref), or 1 mM lysine (Lys), cysteine (Cys), arginine (Arg), tyrosine (Tyr), histidine (His), threonine (Thr), or aspartic acid (Asp). The error bars show the standard deviation of triplicate samples. The dashed line indicates the value for the Ref solution. Asterisks show any statistically significant differences to the Ref solution (* - $p < 0.05$; *** - $p < 0.001$).

protons. The surface pH can then influence the corrosion process, facilitate complexation with chloride ions (see Fig. 3), or result in protonation-induced dissolution¹⁰ of Cu oxides.

The kinetics of adsorption are also essential to understand the experimental data (as opposed to solution equilibrium modelling). Adsorption is discussed below.

Release of Fe, Cr, Ni, and Mo from stainless steel under naturally aerated conditions.—Ligand-induced metal release from stainless steel at neutral pH has been reported for a wide variety of organic molecules and proteins previously,^{17,19,20,24–26,47} however, under different experimental conditions than in this study for Cu. Hence, we compared the release of the main alloying elements from stainless steel under similar conditions as for Cu above. Figure 5 shows the determined released amount of Fe, Cr, Ni, and Mo from the 316 L coupons after 24 h exposure in the various solutions at pH 7.4 and 37 °C. Generally, the amount of released metals (total) was about 1,000-fold lower than for the Cu coupons under similar exposure conditions. The low amount of released metals and the proportion between the released metals (preferential release of Fe, non-preferential release of Cr and Ni) strongly indicate passive conditions (no active corrosion).⁴⁷ The amino acids affected the release of Cr most, with an increase up to 50-fold (histidine), but only lysine resulted in a statistically significant increase (20-fold). In

contrast, the Fe release was only increased up to 5-fold (lysine) and only statistically significant for cysteine (2-fold). The release of Ni and Mo was not statistically significantly affected and increased at most 3-fold (Ni release for histidine).

Despite known reactions between all these amino acids and Fe and Cr species in the database, JESS predicted no difference in solubility for Fe and Cr at pH 7.4, pe 5, 25 °C for these different solutions. It predicted that the predominant species would be $\alpha\text{-Fe}_2\text{O}_3$ (s) in all cases for Fe and CrOOH (s) in all cases for Cr. In contrast, it predicted a clear solution dependence for Ni (Table A-III), with the highest solubility for histidine, aspartic acid, tyrosine, and cysteine and the lowest solubility for the reference solution without amino acids. However, as Ni was unavailable on the surface (see next section), it could not react with the amino acids.

Surface analysis of stainless steel and copper surfaces after one-day exposure to various solutions with and without amino acids.—To verify amino acid adsorption on the metal coupons, XPS analysis was conducted on both stainless steel and Cu coupons for selected amino acids and the reference solution after the one-day exposure (Figs. 4 and 5), with relevant high-resolution peaks shown in Figs. A-3–A-12. The C 1s peak originates from both adventitious carbon and any adsorbed amino acids and consisted of peaks at 284.8 eV attributed to the C–C and C–H bonds,^{48–50} a peak at

286.3 ± 0.06 eV (denoted C2) assigned to peptidic residues, C–O, and C–N bonds,^{48–50} a peak at 287.8 ± 0.06 eV (denoted C3) assigned to N–C=O and C=O bonds,^{48,50} and a peak at 288.8 ± 0.11 eV (denoted C4) assigned to O–C=O bonds.^{48,50} Table I displays the ratio of the sum of the latter three peaks (C2+C3+C4) to the total C 1s peak. All coupons exposed to amino acids show a higher ratio than those exposed to the reference solution and an unexposed coupon. For cysteine, histidine, and arginine, the difference is statistically significant for stainless steel coupons. Sulfur was identified in the wide spectrum (Fig. S4) only in the case of cysteine (the only investigated amino acid containing a thiol group) but not in any other case, which is also indicative of its adsorption.

Similar to previous studies of 316 L in non-aggressive environments (under passive conditions),⁵¹ metal peaks for Ni, Cr, Fe, and Mo were detectable in all cases. This means that the surface oxide and adsorbed layer did not exceed the information depth of XPS (7–10 nm). The ratio between the metal and oxide peaks remained relatively stable for all conditions. Similar to previous work on 316 L and similar grades,^{51,52} Ni was only detected in its metallic form,⁴⁰ which means it was not a component of the surface oxide of stainless steel. Throughout all conditions, and with no significant difference before and after exposure to the different solutions, the surface oxide was composed of oxidized Fe (63 ± 5.7 at%), Cr (35 ± 5.9 at%), and Mo (1.9 ± 0.45 at%).

Hence, for 316 L coupons, there was no significant change in the surface oxide composition and clear signs of amino acid adsorption. In contrast, Cu coupons showed only slight signs of amino acid adsorption (Table I and Figs. A-6 and A-11). A lower degree of amino acid adsorption on a more reactive metal is in line with earlier observations on protein adsorption on Cu and 316 L measured by quartz crystal microbalance.⁵³ While there seemed to be less adsorption of the amino acids, the oxide changes for Cu coupons were far more significant. Metallic Cu was detected after 24 h exposure (naturally aerated, 37 °C, 9 g l⁻¹, 5 mM MES, pH 7.4) to the reference solution without amino acids, indicative of an oxide thinner than the XPS detection depth (7–10 nm). No metallic Cu was detected for Cu coupons exposed to 1 mM tyrosine, threonine, or serine, Figs. A-3, A-4. For the Cu specimens exposed to threonine, there was a higher fraction of divalent Cu species, as evident from the larger shake-up peak (peak B) in the Cu 2p_{3/2} peak³⁹ (Fig. A-3) and the Cu L₃M_{4,5}M_{4,5} peak-fitting results (Fig. A-4). From the O 1s peaks (Fig. A-6) and Cu L₃M_{4,5}M_{4,5} (Fig. A-4) peaks, it was evident that most of the divalent Cu was in the form of Cu(OH)₂ after exposure to the threonine-containing solution.

Hence, XPS results suggest that threonine, serine, and tyrosine under the experimental conditions cause some oxidation for the Cu coupons, in contrast to the reference solution and 316 L.

Overall discussion, limitations and further research.—

Adsorption of amino acids on surfaces is influenced by the surface charge and hydrophobicity, the ionic strength of the solution (affecting the double layer thickness), the amino acid concentration, solution pH and temperature.^{54–56} The ionic strength of the investigated solution in this study was high, which reduces the importance of electrostatic interactions.^{54,57} This might explain why three positively charged amino acids (lysine, histidine, and arginine) were able to induce among the highest Cu release despite the surface charge of Cu is to be expected slightly positive at pH 7.4.⁵⁸ However, a recent review concluded that published values of isoelectric points for Cu, copper oxides and hydroxides are too scattered to draw any conclusions on their reliability.⁵⁹ Future studies should investigate whether any electrostatic interactions play a role in the observed amino acid-induced Cu release and corrosion. For stainless steel, which is negatively charged at pH 7.4,^{23,53,57,60–62} the relatively high observed release for the positively charged lysine and histidine makes sense. However, the positively charged arginine did not induce any increased release.

Cysteine is a particular case, as it is the only investigated amino acid with a thiol functional group in this study. Cysteine increased the Cu

release from Cu and the Fe release from 316 L in this study. Cu (both as ions and as a metal surface) interactions with cysteine are known from the literature^{63–67} and strongly predicted by the chemical speciation modelling in this study (relative solubility of 100% at pH 7.4). For stainless steel, iron, and chromium, strong cysteine interactions were not predicted by the chemical speciation modelling at pH 7.4, and literature data is more scarce; however, strong Fe(II)-cysteine interactions have been shown for the gas phase.⁶⁸

This study is a precursor and bridge toward understanding peptide and protein-induced corrosion of Cu and other metals. Future studies should investigate other pure metals rather than an alloy. However, stainless steel should be examined under slightly more aggressive conditions, such as somewhat lower pH or higher amino acid concentration, as it remained entirely in passive conditions and did not change surface composition or thickness. Previous studies with proteins at pH 7.4²³ or citrate species at pH 4.5²⁰ have shown that metal release, including Ni release, which is indicative of oxide defects, from stainless steel 316 L is affected by these ligands.

This study applied a phosphate-free buffer (MES buffer) to avoid metal precipitation.^{4,35} This has previously been shown, both by modelling and experimental data,^{4,69,70} to be essential to avoid underestimation of Cu release in physiological environments. In addition, the incorporation of phosphates, which slow down corrosion, in a surface layer on Fe has been shown in simulated media containing phosphates.⁷¹ For stainless steel, it has been reported that threonine and lysine (at 10–100 mM) inhibited corrosion even at neutral pH (with phosphates), as determined by potentiodynamic polarization.⁷² However, a closer look at that work suggests that a pre-passivation from the amino acids caused this effect. Hence, to our knowledge, this is the first study presenting metal release and corrosion data for Cu in neutral pH in the presence of amino acids and the absence of phosphates.

Conclusions

The investigated amino acids at 1 mM and pH 7.4 in 9 g l⁻¹ NaCl generally increased the corrosion current density and decreased the corrosion potential of Cu compared with the reference solution not containing amino acids. This was also shown by increased oxide thickness using surface analysis. This trend was independent of aeration. All selected amino acids (lysine, cysteine, arginine, tyrosine, histidine, threonine, tryptophan, serine, glutamic acid, glycine) increased the release of Cu during a 24 h exposure in naturally aerated conditions at pH 7.4 and 37 °C, at most 18-fold. Equilibrium chemical speciation modelling (in solution) predicted the general trend but not the exact trend among amino acids. Stainless steel maintained passive conditions and did not change its surface oxide composition or thickness during a similar 24 h exposure. Nevertheless, the Fe release was significantly higher in 1 mM cysteine, and the Cr release was 52-fold higher in 1 mM lysine than in the reference solution. The surface analysis confirmed the adsorption of amino acids after the 24 h exposure and rinsing in all cases. Equilibrium chemical speciation modelling could predict the general higher release for Cu in the presence of amino acids and its independence from oxygen. However, it did not predict the increased Fe and Cr release from 316 L.

Acknowledgments

We want to acknowledge funding from the Canada Research Chairs Program (#950–233099), startup funds at Western University, Canada (Dept. Chemistry, 2020), Wolfe-Western fellowship, Canada (Grant No.: 2020), and the Natural Sciences and Engineering Research Council of Canada (RGPIN-2021–03997, DGDND-2021–03997, Undergraduate Student Research Awards—Vander Zee 2021).

We highly acknowledge Dr. Peter May, Murdoch University, Australia, for support regarding the Joint Expert Speciation System.

Appendix

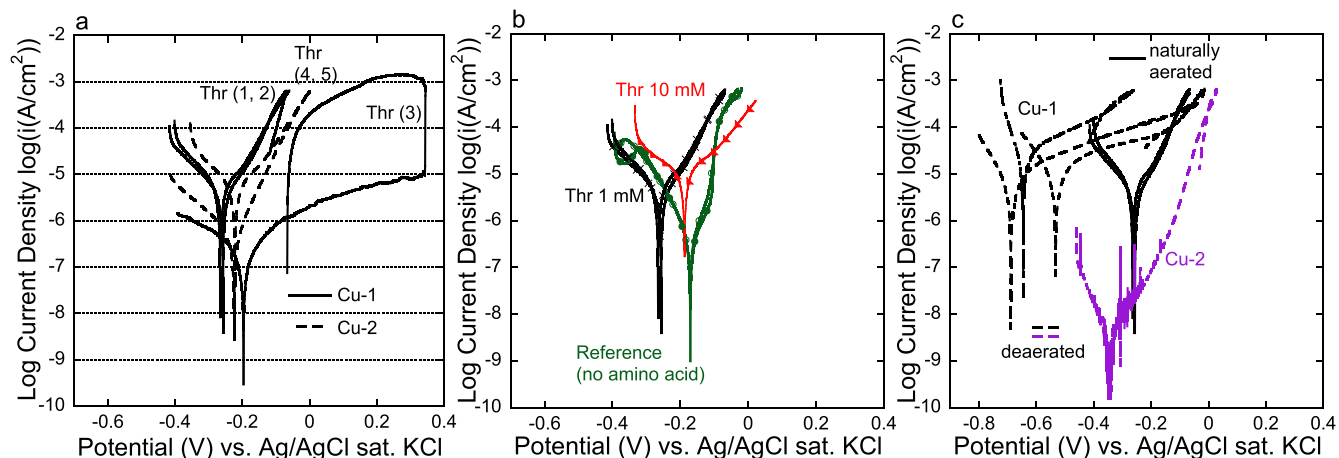


Figure A-1. Potentiodynamic polarization curves and corrosion current densities of Cu specimens (Cu-1 and Cu-2) exposed to aerated and deaerated solutions at pH 7.40 and 25 °C with varying concentrations of threonine. a) Polished Cu specimens (Cu-1 and Cu-2, as indicated) were desiccated for 24 h before immersion in the naturally aerated solutions of 9 g l⁻¹ NaCl, 5 mM MES buffer, and 1 mM threonine. b) Polished and desiccated Cu-1 for 24 h before immersion in 9 g l⁻¹ NaCl, 5 mM MES buffer, and either 0 (reference, duplicate), 1 (duplicate) or 10 mM of threonine under naturally aerated conditions. c) Deaerated conditions (dashed lines in c): Freshly polished Cu specimen (Cu-1 and Cu-2) directly immersed in pre-purged and purged electrolyte. Naturally aerated conditions are indicated as solid lines representing polished Cu specimens (Cu-1), 24 h desiccated before immersion in the non-purged electrolyte. The electrolyte composition was as in a).

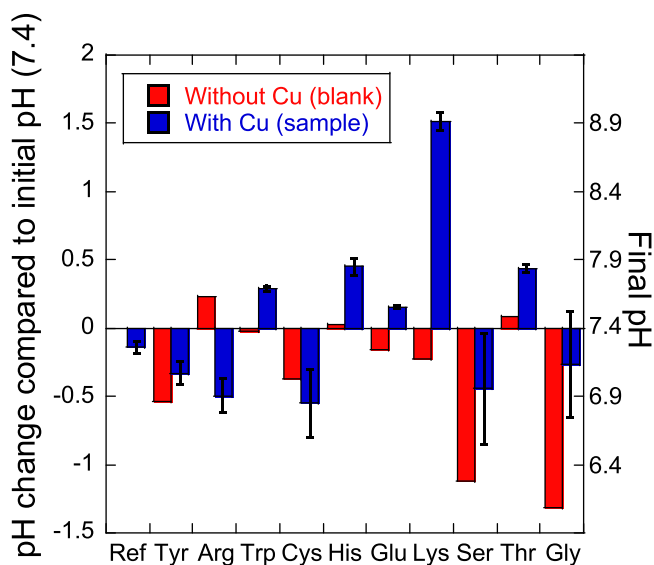


Figure A-2. Change in pH (left axis) and final pH (right axis) after 24 h under naturally aerated exposure at 37 ± 0.5 °C in 9 g l⁻¹ NaCl, 5 mM MES buffer, pH 7.4, containing no amino acid (Ref), or 1 mM tyrosine (Tyr), arginine (Arg), tryptophan (Trp), cysteine (Cys), histidine (His), glutamic acid (Glu), lysine (Lys), serine (Ser), threonine (Thr), or glycine (Gly), for the blank solution without any Cu coupon (red) or the triplicate samples with Cu coupons (blue, error bars show the standard deviation of triplicate samples, except for Arg, which were duplicate samples). The pH of the blank solution of the Ref solution did not change during the 24 h.

Table A-1. Determined aqueous (released) Cu ($\mu\text{g}/\text{cm}^2$) after 24 h under naturally aerated exposure of Cu coupons (Cu-3) at 37 ± 0.5 °C in 9 g l⁻¹ NaCl, 5 mM MES buffer, pH 7.4, containing no amino acid (Ref), or 1 mM amino acid, as indicated. Average and standard deviation values of triplicate samples. Asterisks show any statistically significant differences to the Ref solution (* - p < 0.05; ** - p < 0.01, *** - p < 0.001).

Amino acid	Cu release/surface area ($\mu\text{g}/\text{cm}^2$)
Ref ^{a)}	13 ± 1
Lysine	144 ± 11 ^{**}
Cysteine	242 ± 44 [*]
Arginine ^{b)}	123 ± 3 ^{**}
Tyrosine	137 ± 3 [*]
Histidine	76 ± 4 ^{***}
Threonine	26 ± 4 [*]
Tryptophan	86 ± 11 ^{**}
Glutamic acid	46 ± 3 ^{**}
Serine	18 ± 2 [*]
Glycine	29 ± 6 [*]

a) for Cu-2, this reference solution value was 7.3 ± 4.5 $\mu\text{g cm}^{-12}$. b) only two replicates.

Table A-II. Aqueous species as a percentage of 1 mM total Cu in 9 g l⁻¹ NaCl, containing no amino acid or 1 mM of various amino acids, at pH 7.4, 25 °C, 1 atm pressure, and pe 5. Corresponding equilibrium JESS data to Figs. 1, 3 and S1. In the case of cysteine, the species (Cu^I₅-Cys^{-II}₄)³⁻ was excluded due to a numerical error.

Solution	Ref	Lys	Cys	Arg	Tyr	His	Thr	Trp	Glu	Ser	Gly
% aqueous Solution	0	33	100	78	46	100	70	45	37	54	37
% aqueous Solution	His+Tyr	His+Trp	His+Thr	His+Ser							
	100	100	100	100							

Table A-III. Five predominant Ni species, based on JESS, for 1 mM total Ni in 9 g l⁻¹ NaCl, 25 °C, 1 atm pressure, pe 5, and pH 7.4, and either no or 1 mM of an amino acid added, as indicated. Values are given in % (of 1 mM total Ni). The valence state is two in all cases for Ni. s—solid; Arg—arginine; Asp—aspartic acid; Cys—cysteine; His—histidine; Lys—lysine; Ser—serine; Thr—threonine; Trp—tryptophan; Tyr—tyrosine. All species that do not indicate a solid species are aqueous.

No amino acid (reference solution)					
% of 1 mM Ni Species	86	8	4	2	—
	Ni(OH) ₂ (s)	Ni ²⁺	NiCl ⁺	NiCl ₂	—
1 mM lysine					
% of 1 mM Ni Species	77	9	8	4	2
	Ni(OH) ₂ (s)	(NiH-Lys ^{-I}) ²⁺	Ni ²⁺	NiCl ⁺	(NiH ₂ -Lys ^{-I}) ²⁺
1 mM cysteine					
% of 1 mM Ni Species	38	26	24	8	4
	(Ni-Cys ^{-II}) ₂ ²⁻	Ni-Cys ^{-II}	Ni(OH) ₂ (s)	Ni ²⁺	NiCl ⁺
1 mM arginine					
% of 1 mM Ni Species	60	23	8	5	4
	Ni(OH) ₂ (s)	(Ni-Arg ^{-I}) ⁺	Ni ²⁺	Ni-Arg ^{-I} ₂	NiCl ⁺
1 mM tyrosine					
% of 1 mM Ni Species	33	33	22	8	4
	(NiH ₂ -Tyr ^{-II}) ²⁺	(NiH ₄ -Tyr ^{-II}) ²⁺	Ni(OH) ₂ (s)	Ni ²⁺	NiCl ⁺
1 mM histidine					
% of 1 mM Ni Species	80	10	6	3	1
	(Ni-His ^{-I}) ⁺	Ni-His ^{-I} ₂	Ni ²⁺	NiCl ⁺	NiCl ₂
1 mM threonine					
% of 1 mM Ni Species	39	37	12	8	4
	Ni(OH) ₂ (s)	(Ni-Thr ^{-I}) ⁺	Ni-Thr ^{-I} ₂	Ni ²⁺	NiCl ⁺
1 mM aspartic acid					
% of 1 mM Ni Species	89	5	3	2	1
	Ni-Asp ^{-II}	Ni ²⁺	NiCl ⁺	(Ni-Asp ^{-II}) ₂ ²⁻	NiCl ₂

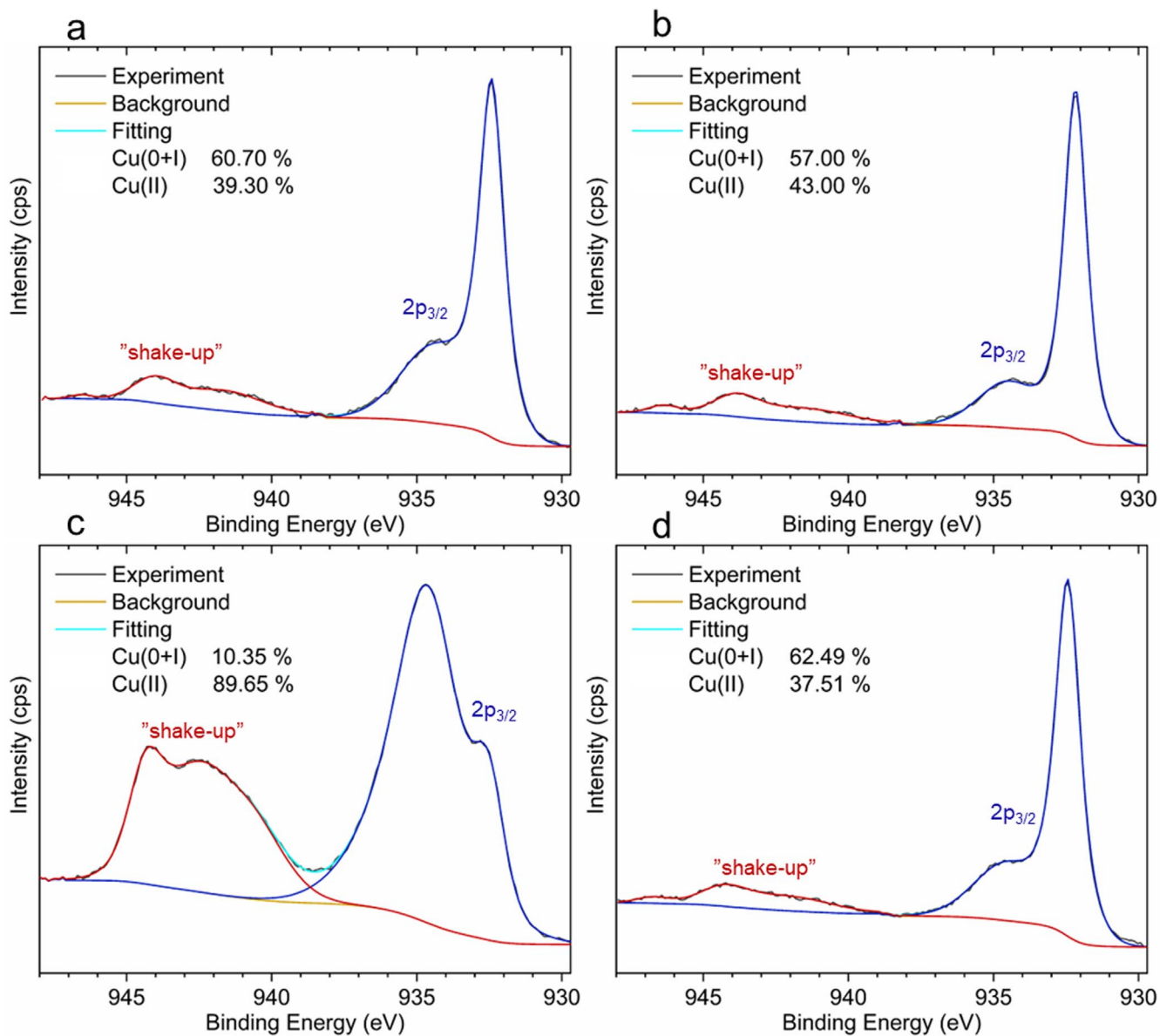


Figure A-3. High-resolution Cu $2p_{3/2}$ peaks of surfaces of Cu coupons (Cu-3) after immersion for 24 h under naturally aerated exposure at 37 ± 0.5 °C in 9 g l^{-1} NaCl, 0.5 mM MES buffer, pH 7.4, containing no amino acid (a), or 1 mM serine (b), 1 mM threonine (c), or 1 mM tyrosine (d), measured using XPS. Cu(0 + I) and Cu(II) values were calculated from the main $2p_{3/2}$ (blue line) and shake-up structure peak (red line) areas using the calculations presented previously.³⁹

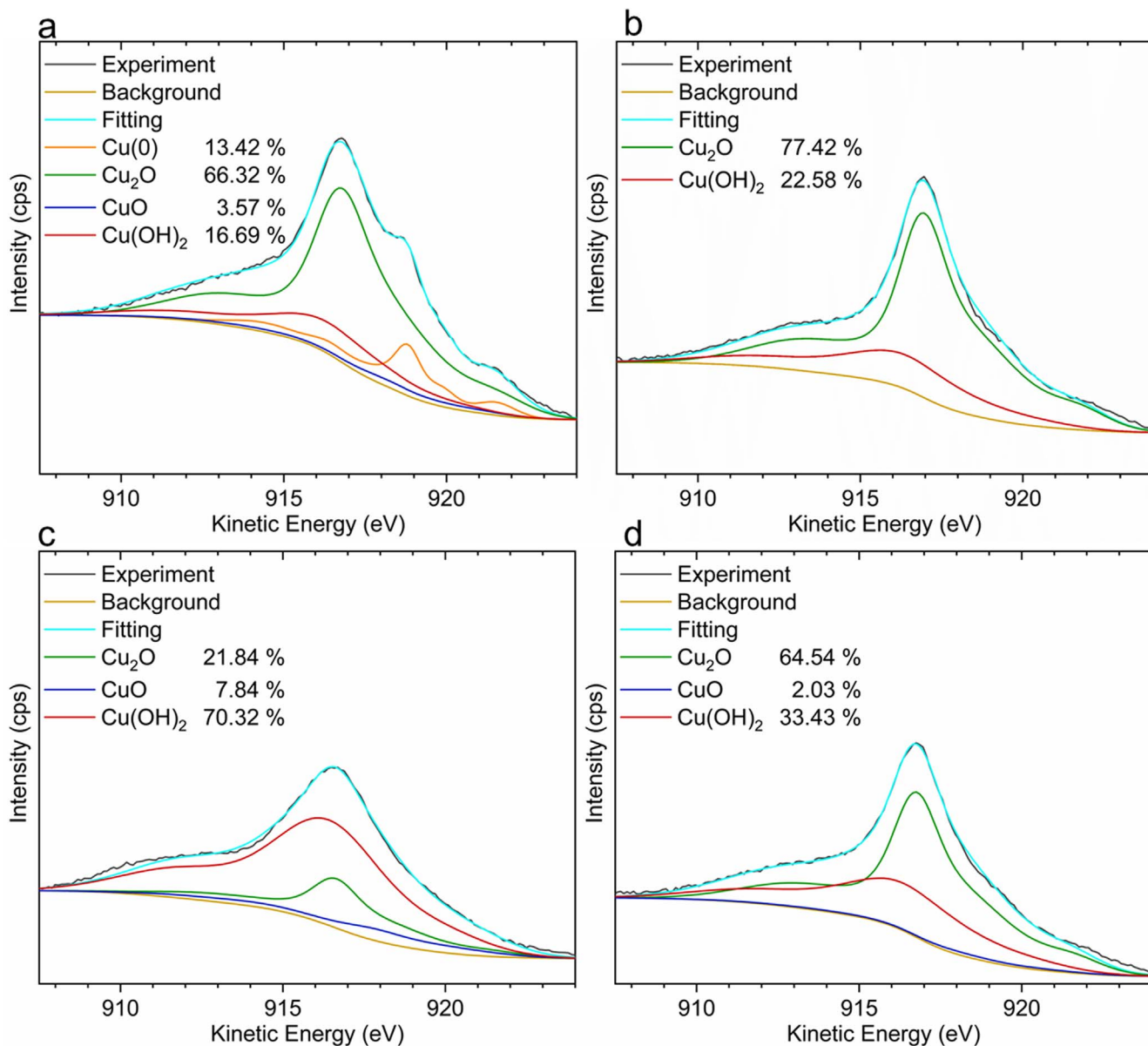


Figure A-4. High-resolution Cu $L_{3,4,5}M_{4,5}$ peaks of surfaces of Cu coupons (Cu-3) after immersion for 24 h under naturally aerated exposure at 37 ± 0.5 °C in 9 g l^{-1} NaCl, 0.5 mM MES buffer, pH 7.4, containing no amino acid (a), or 1 mM serine (b), 1 mM threonine (c), or 1 mM tyrosine (d), measured using XPS.

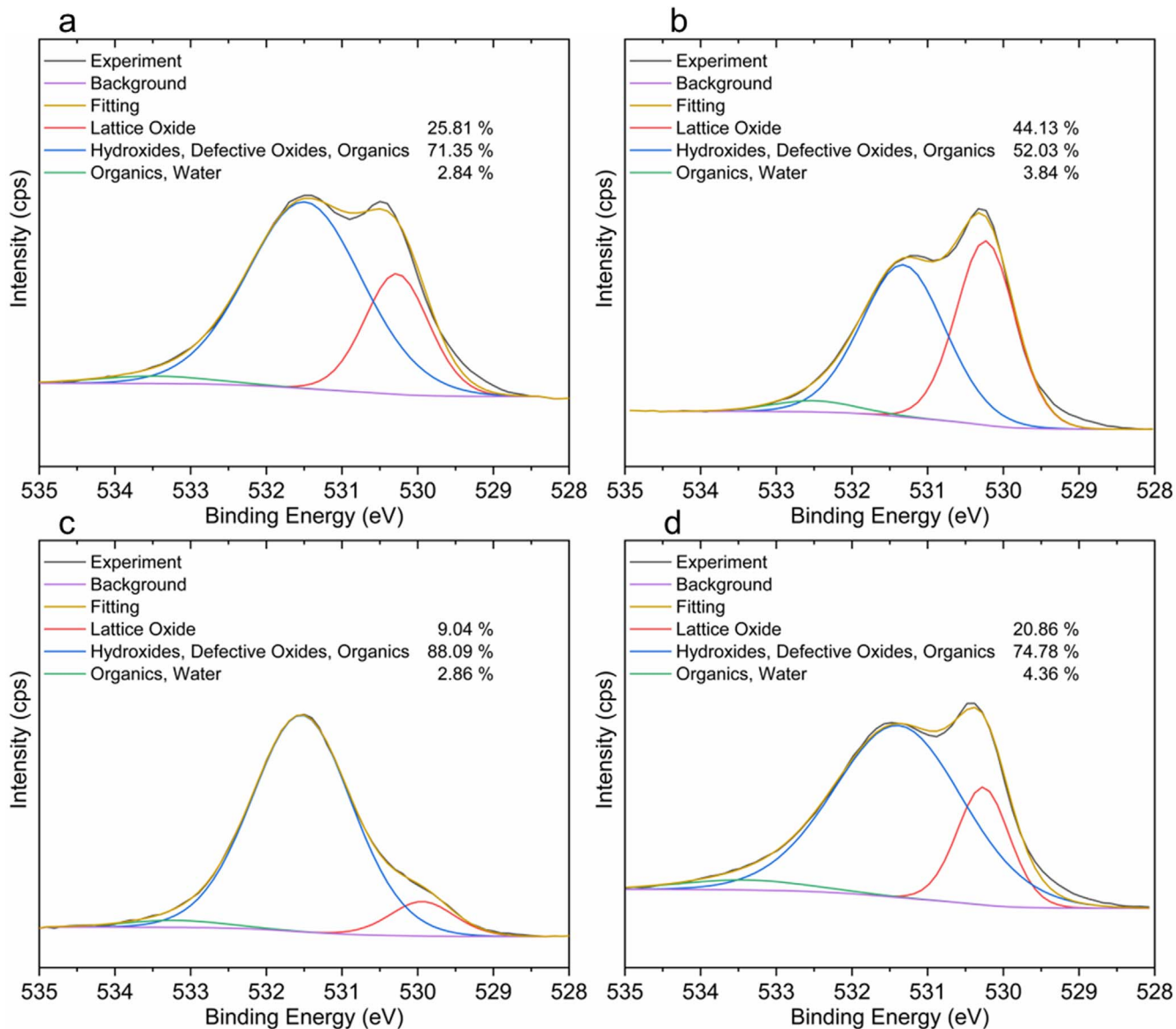


Figure A.5. High-resolution O 1s peaks of surfaces of Cu coupons (Cu-3) after immersion for 24 h under naturally aerated exposure at 37 ± 0.5 °C in 9 g l^{-1} NaCl, 0.5 mM MES buffer, pH 7.4, containing no amino acid (a), or 1 mM serine (b), 1 mM threonine (c), or 1 mM tyrosine (d), measured using XPS.

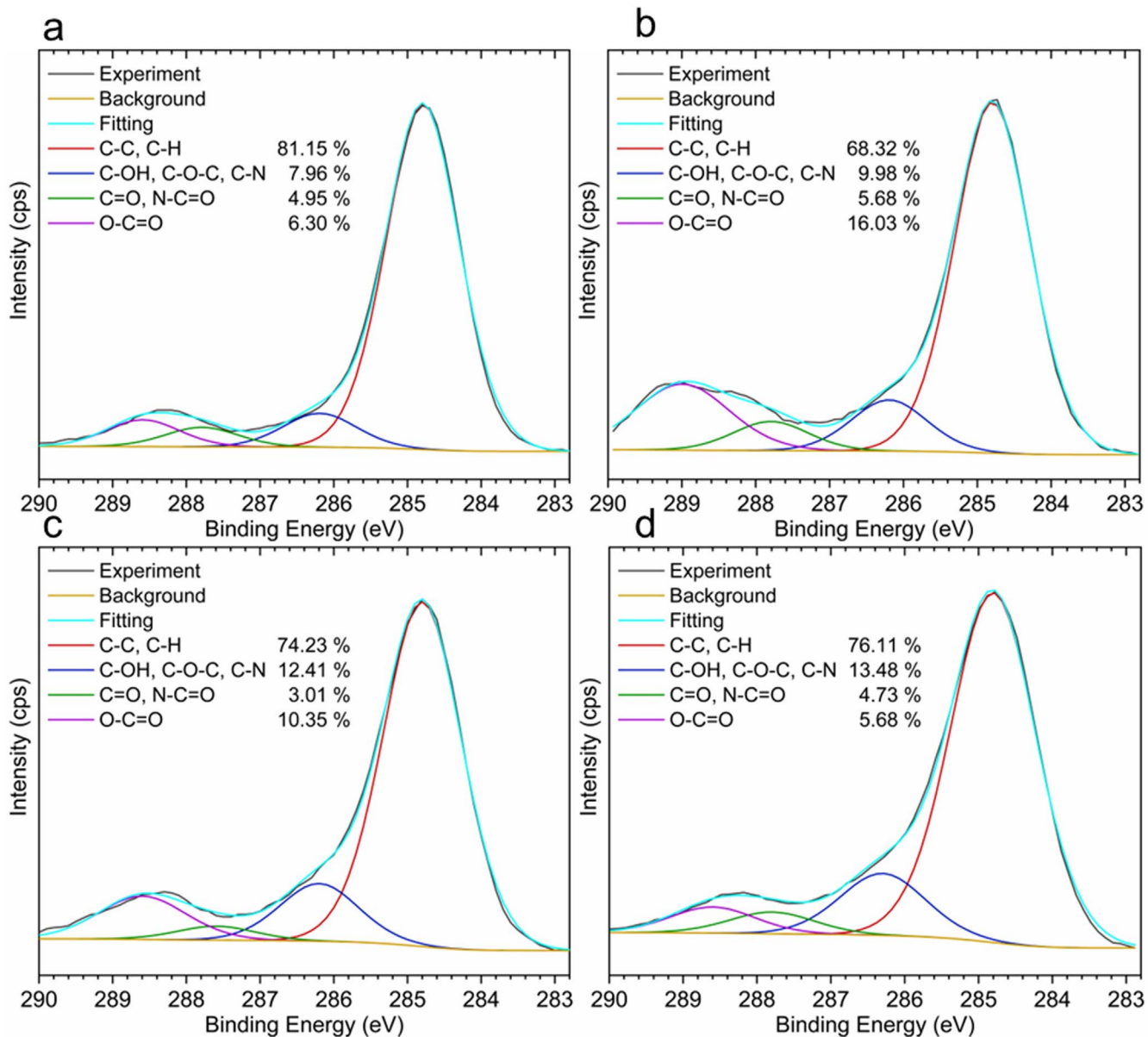


Figure A-6. High-resolution C 1s peaks of surfaces of Cu coupons (Cu-3) after immersion for 24 h under naturally aerated exposure at 37 ± 0.5 °C in 9 g l^{-1} NaCl, 0.5 mM MES buffer, pH 7.4, containing no amino acid (a), or 1 mM serine (b), 1 mM threonine (c), or 1 mM tyrosine (d), measured using XPS.

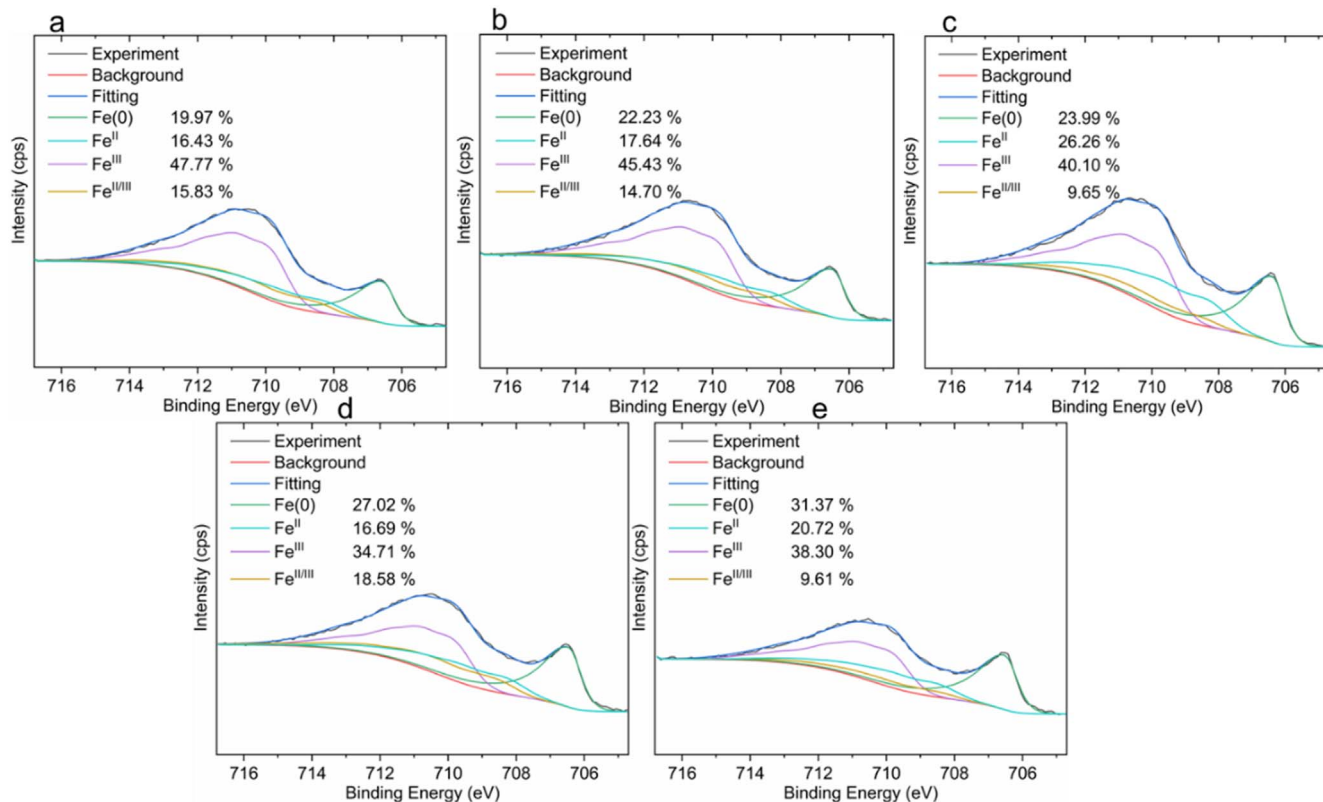


Figure A-7. Representative high-resolution Fe 2p_{3/2} peaks of unexposed (a) and exposed surfaces of 316 L coupons after immersion for 24 h under naturally aerated exposure at 37 ± 0.5 °C in 9 g l⁻¹ NaCl, 0.5 mM MES buffer, pH 7.4, containing no amino acid (b), or 1 mM cysteine (c), 1 mM threonine (d), or 1 mM tyrosine (e), measured using XPS.

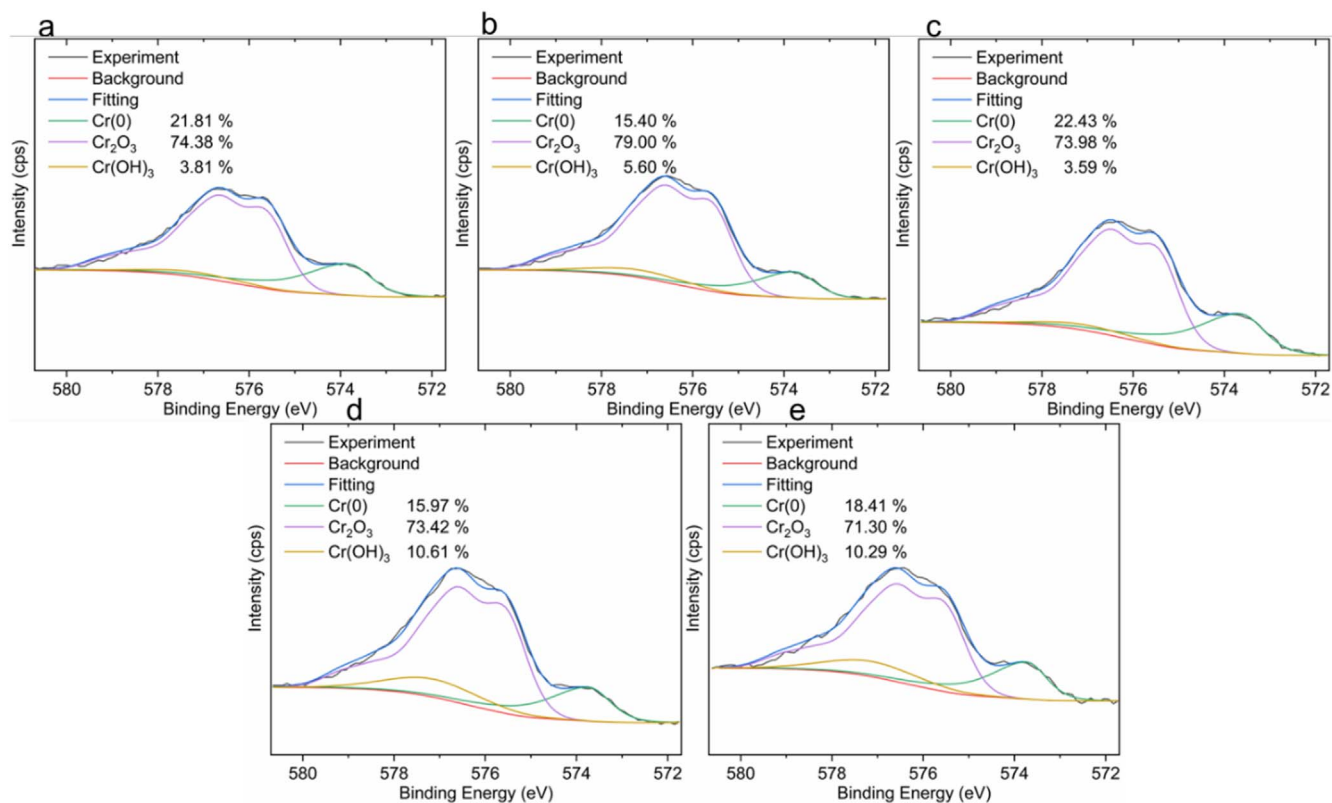


Figure A-8. Representative high-resolution Cr 2p_{3/2} peaks of unexposed (a) and exposed surfaces of 316 L coupons after immersion for 24 h under naturally aerated exposure at 37 ± 0.5 °C in 9 g l⁻¹ NaCl, 0.5 mM MES buffer, pH 7.4, containing no amino acid (b), or 1 mM cysteine (c), 1 mM threonine (d), or 1 mM tyrosine (e), measured using XPS.

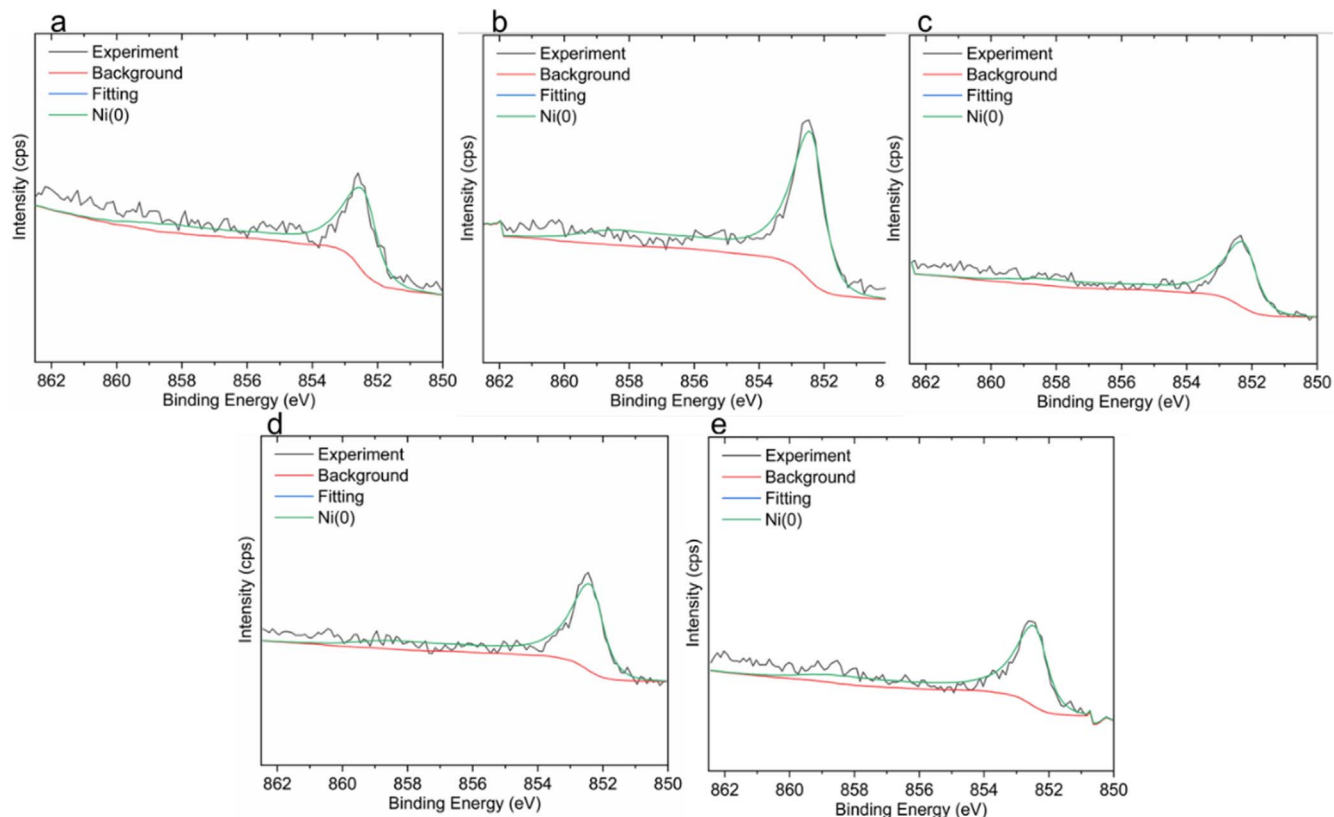


Figure A-9. Representative high-resolution Ni 2p_{3/2} peaks of unexposed (a) and exposed surfaces of 316 L coupons after immersion for 24 h under naturally aerated exposure at 37 ± 0.5 °C in 9 g l⁻¹ NaCl, 0.5 mM MES buffer, pH 7.4, containing no amino acid (b), or 1 mM cysteine (c), 1 mM threonine (d), or 1 mM tyrosine (e), measured using XPS.

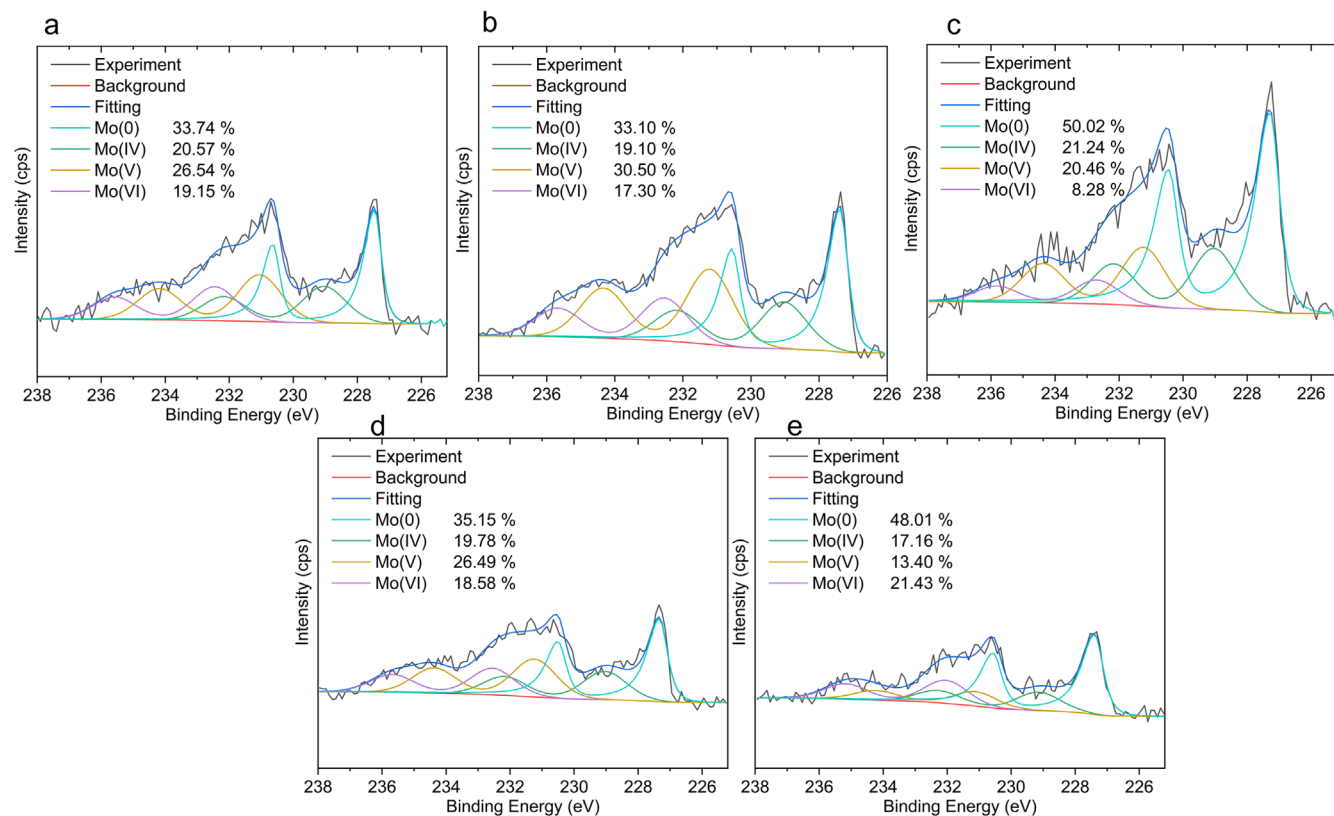


Figure A-10. Representative high-resolution Mo 3d_{5/2} peaks of unexposed (a) and exposed surfaces of 316 L coupons after immersion for 24 h under naturally aerated exposure at 37 ± 0.5 °C in 9 g l⁻¹ NaCl, 0.5 mM MES buffer, pH 7.4, containing no amino acid (b), or 1 mM cysteine (c), 1 mM threonine (d), or 1 mM tyrosine (e), measured using XPS.

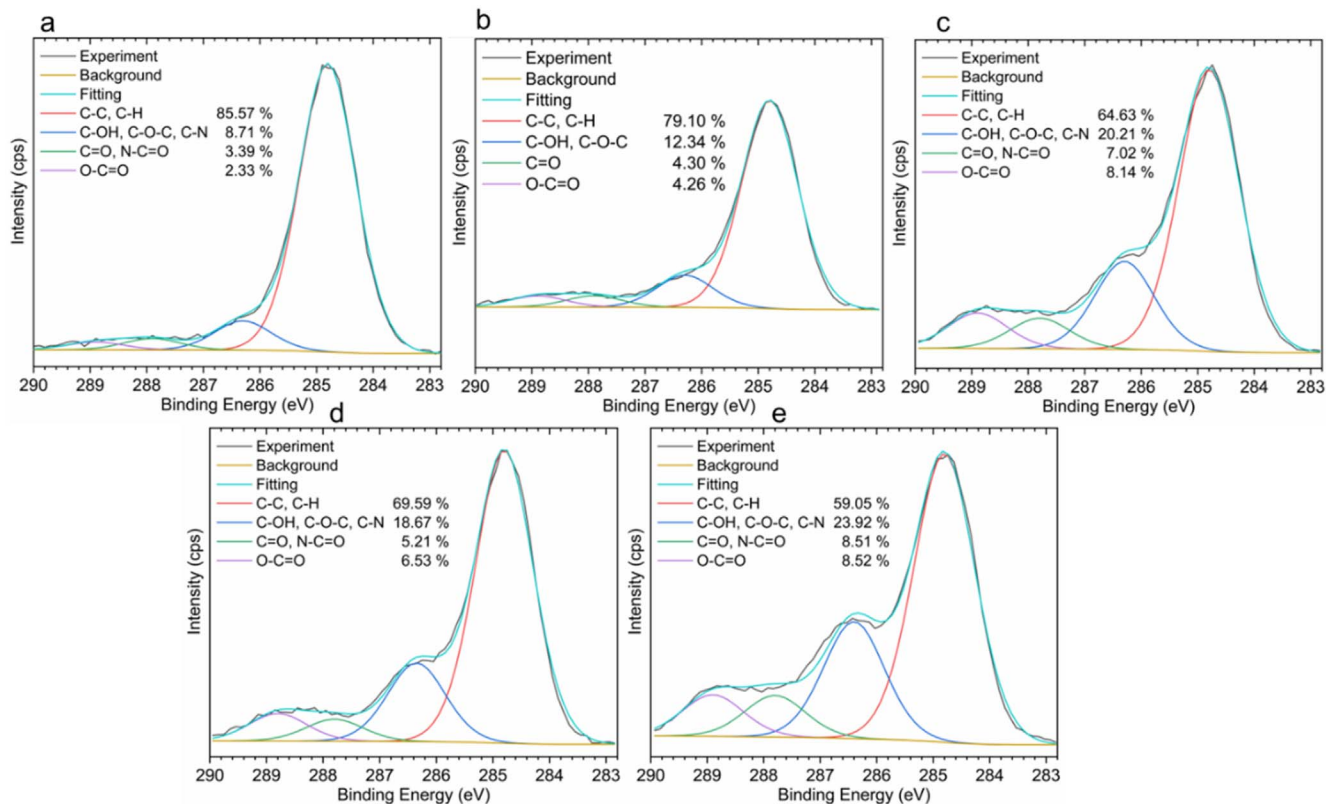


Figure A-11. Representative high-resolution C 1s peaks of unexposed (a) and exposed surfaces of 316 L coupons after immersion for 24 h under naturally aerated exposure at 37 ± 0.5 °C in 9 g l^{-1} NaCl, 0.5 mM MES buffer, pH 7.4, containing no amino acid (b), or 1 mM cysteine (c), 1 mM threonine (d), or 1 mM tyrosine (e), measured using XPS.

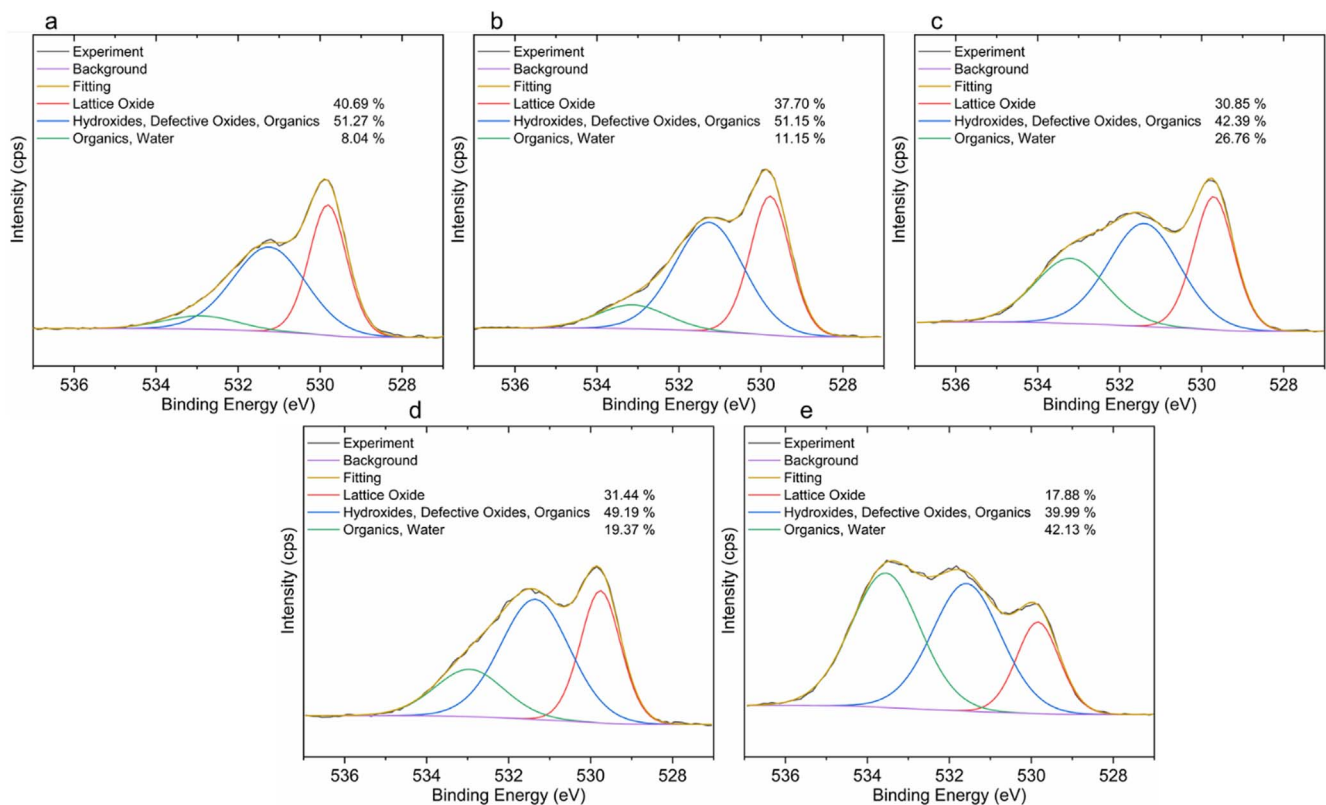


Figure A-12. Representative high-resolution O 1s peaks of surfaces of unexposed (a) and exposed 316 L coupons after immersion for 24 h under naturally aerated exposure at 37 ± 0.5 °C in 9 g l^{-1} NaCl, 0.5 mM MES buffer, pH 7.4, containing no amino acid (b), or 1 mM cysteine (c), 1 mM threonine (d), or 1 mM tyrosine (e), measured using XPS.

ORCID

Sina Matin  <https://orcid.org/0000-0002-5339-9313>
 Jeffrey D. Henderson  <https://orcid.org/0000-0001-7415-756X>
 Jonas F. Hedberg  <https://orcid.org/0000-0003-2100-8864>
 James J. Noël  <https://orcid.org/0000-0003-3467-4778>
 Yolanda S. Hedberg  <https://orcid.org/0000-0003-2145-3650>

References

- D. Mitra, E.-T. Kang, and K. G. Neoh, *ACS Appl. Mater. Interfaces*, **12**, 21159 (2020).
- M. E. Ortiz and H. B. Croxatto, *Contraception*, **75**, S16 (2007).
- A. Kessler, J. Hedberg, E. Blomberg, and I. Odnevall, *Nanomaterials*, **12**, 1922 (2022).
- J. Hedberg, H. L. Karlsson, Y. Hedberg, E. Blomberg, and I. Odnevall Wallinder, *Colloid Surface B*, **141**, 291 (2016).
- P. M. Roos, O. Vesterberg, T. Syversen, T. P. Flaten, and M. Nordberg, *Biol. Trace Elem. Res.*, **151**, 159 (2013).
- A. Nicoletti, R. Vasta, V. Venti, G. Mostile, S. Lo Fermo, F. Patti, R. Scillieri, D. De Cicco, P. Volanti, and R. Marziolo, *European Journal of Neurology*, **23**, 964 (2016).
- G. J. Brewer, *Experimental Biology and Medicine*, **232**, 323 (2007).
- D. L. Sparks and B. G. Schreurs, *Proc. Natl. Acad. Sci.*, **100**, 11065 (2003).
- Z. Wang, A. von dem Bussche, P. K. Kabadi, A. B. Kane, and R. H. Hurt, *ACS Nano*, **7**, 8715 (2013).
- W. Stumm and R. Wollast, *Rev. Geophys.*, **28**, 53 (1990).
- G. L. Mendonça, S. N. Costa, V. N. Freire, P. N. Casciano, A. N. Correia, and P. de Lima-Neto, *Corros. Sci.*, **115**, 41 (2017).
- M. A. Amin and K. Khaled, *Corros. Sci.*, **52**, 1194 (2010).
- D.-Q. Zhang, Q.-R. Cai, L.-X. Gao, and K. Y. Lee, *Corros. Sci.*, **50**, 3615 (2008).
- D.-Q. Zhang, Q.-R. Cai, X.-M. He, L.-X. Gao, and G.-D. Zhou, *Mater. Chem. Phys.*, **112**, 353 (2008).
- D.-Q. Zhang, B. Xie, L.-X. Gao, Q.-R. Cai, H. G. Joo, and K. Y. Lee, *Thin Solid Films*, **520**, 356 (2011).
- D.-Q. Zhang, L.-X. Gao, and G.-D. Zhou, *J. Appl. Electrochem.*, **35**, 1081 (2005).
- N. Mazinanian and Y. S. Hedberg, *J. Electrochem. Soc.*, **163**, C686 (2016).
- I. Milošev, *J. Appl. Electrochem.*, **32**, 311 (2002).
- N. S. Al-Mamun, K. Mairaj Deen, W. Haider, E. Asselin, and I. Shabib, *Additive Manufacturing*, **34**, 101237 (2020).
- Y. Hedberg, J. Hedberg, Y. Liu, and I. Odnevall Wallinder, *BioMetals*, **24**, 1099 (2011).
- Y. Okazaki and E. Gotoh, *Biomaterials*, **26**, 11 (2005).
- A. Kocijan, I. Milošev, and B. Pihlar, *J. Mater. Sci.-Mater. M.*, **14**, 69 (2003).
- Y. Hedberg, X. Wang, J. Hedberg, M. Lundin, E. Blomberg, and I. Odnevall Wallinder, *J. Mater. Sci.-Mater. M.*, **24**, 1015 (2013).
- Y. S. Hedberg, *npj Materials Degradation*, **2**, 26 (2018).
- M. Talha, Y. Ma, Y. Lin, A. K. Mandal, O. P. Sinha, and X. Kong, *Colloid Surface B*, **197**, 111407 (2021).
- M. Talha, Y. Ma, Y. Lin, A. Singh, W. Liu, and X. Kong, *New J. Chem.*, **43**, 1943 (2019).
- J. A. Tainer, V. A. Roberts, and E. D. Getzoff, *Curr. Opin. Biotech.*, **3**, 378 (1992).
- R. F. Carbonaro, B. N. Gray, C. F. Whitehead, and A. T. Stone, *Geochim. Cosmochim. Ac.*, **72**, 3241 (2008).
- Y. Zhang, N. Kallay, and E. Matijevic, *Langmuir*, **1**, 201 (1985).
- Y. Hedberg, M.-E. Karlsson, E. Blomberg, I. Odnevall Wallinder, and J. Hedberg, *Colloid Surface B*, **122**, 216 (2014).
- C. J. Beverung, C. J. Radke, and H. W. Blanch, *Biophys. Chem.*, **81**, 59 (1999).
- Y. Hedberg and K. Midander, *Mater. Lett.*, **122**, 223 (2014).
- U. Schwertmann, *Plant Soil*, **130**, 1 (1991).
- Y. S. Hedberg, M. Žnidaršič, G. Herting, I. Milošev, and I. Odnevall Wallinder, *J. Biomed. Mater. Res. B*, **107**, 858 (2019).
- H. E. Mash, Y.-P. Chin, L. Sigg, R. Hari, and H. Xue, *Anal. Chem.*, **75**, 671 (2003).
- P. M. May, *Appl. Geochem.*, **55**, 3 (2015).
- P. M. May and D. Rowland, *J. Chem. Eng. Data*, **62**, 2481 (2017).
- P. M. May, P. W. Linder, and D. R. Williams, *J. Chem. Soc., Dalton Trans.*, **588** (1977).
- M. C. Biesinger, *Surf. Interface Anal.*, **49**, 1325 (2017).
- M. C. Biesinger, B. P. Payne, A. P. Grosvenor, L. W. M. Lau, A. R. Gerson, and R. S. C. Smart, *Appl. Surf. Sci.*, **257**, 2717 (2011).
- T. Stepan, L. Tété, L. Laundry-Mottiar, E. Romanovskaia, Y. S. Hedberg, H. Danninger, and M. Auinger, *Electrochim. Acta*, **409**, 139923 (2022).
- N. Makarenko, U. Kharchenko, and L. Zemnukhova, *Russ. J. Appl. Chem.*, **84**, 1362 (2011).
- G. K. Gomma and M. H. Wahdan, *Mater. Chem. Phys.*, **39**, 142 (1994).
- K. Barouni, L. Bazzi, R. Salghi, M. Mihit, B. Hammouti, A. Albourine, and S. El Issami, *Mater. Lett.*, **62**, 3325 (2008).
- M. Momeni and J. Wren, *Faraday Discuss.*, **180**, 113 (2015).
- E. Badetti, L. Calgaro, L. Falchi, A. Bonetto, C. Bettiol, B. Leonetti, E. Ambrosi, E. Zendri, and A. Marcomini, *Nanomaterials*, **9**, 792 (2019).
- Y. S. Hedberg and I. Odnevall Wallinder, *Biointerphases*, **11**, 018901 (2016).
- H. Wu, L. Zhuo, Q. He, X. Liao, and B. Shi, *Appl. Catal. A-Gen.*, **366**, 44 (2009).
- A. Ithurbide, I. Frateur, A. Galtayries, and P. Marcus, *Electrochim. Acta*, **53**, 1336 (2007).
- M. C. Biesinger, *Appl. Surf. Sci.*, **597**, 153681 (2022).
- X. Wang, J. Hedberg, H.-Y. Nie, M. C. Biesinger, I. Odnevall, and Y. S. Hedberg, *Mater. Des.*, **215**, 110524 (2022).
- I. Olefjord and L. Wegrelius, *Corros. Sci.*, **31**, 89 (1990).
- M. Lundin, Y. Hedberg, T. Jiang, G. Herting, X. Wang, E. Thormann, E. Blomberg, and I. Odnevall Wallinder, *J. Colloid Interf. Sci.*, **366**, 155 (2012).
- W. Norde and J. Lyklema, *J. Colloid Interf. Sci.*, **66**, 257 (1978).
- W. Norde and J. Lyklema, *J. Colloid Interf. Sci.*, **66**, 266 (1978).
- C. J. van Oss, *Interfacial forces in aqueous media* (Taylor and Francis Group, LLC, Boca Raton) 266 (2006).
- S. Fukuzaki, H. Urano, and K. Nagata, *J. Ferment. Bioeng.*, **80**, 6 (1995).
- N. Kallay, Z. Torbic, M. Golic, and E. Matijevic, *J. Phys. Chem.-US*, **95**, 7028 (1991).
- M. Kosmulski, *Adv. Colloid Interfac.*, **238**, 1 (2016).
- C. Exartier, S. Maximovitch, and B. Baroux, *Corros. Sci.*, **46**, 1777 (2004).
- G. Lefèvre, L. Čerović, S. Milonjić, M. Fédoroff, J. Finne, and A. Jaubertie, *J. Colloid Interf. Sci.*, **337**, 449 (2009).
- N. Kallay, D. Kovacevic, I. Dedic, and V. Tomic, *Corrosion*, **50**, 598 (1994).
- Z. Wu, F. A. Fernandez-Lima, and D. H. Russell, *J. Am. Soc. Mass. Spectrom.*, **21**, 522 (2010).
- E. Mateo Marti, C. Methivier, and C. M. Pradier, *Langmuir*, **20**, 10223 (2004).
- A. Rigo, A. Corazza, M. L. di Paolo, M. Rossetto, R. Ugolini, and M. Scarpa, *J. Inorg. Biochem.*, **98**, 1495 (2004).
- D. Kumar, N. Jain, V. Jain, and B. Rai, *Appl. Surf. Sci.*, **514**, 145905 (2020).
- A. Ihs and B. Liedberg, *J. Colloid Interf. Sci.*, **144**, 282 (1991).
- O. V. Nemirovskiy and M. L. Gross, *J. Am. Soc. Mass. Spectrom.*, **7**, 977 (1996).
- M. B. Valcarce and M. Vázquez, *Corros. Sci.*, **52**, 1413 (2010).
- J. Dartmann, T. Alex, T. Dorsch, E. Schevalje, and K. Johannsen, *Acta Hydroch. Hydrob.*, **32**, 25 (2004).
- H. Dong, F. Lin, A. R. Boccaccini, and S. Virtanen, *Corros. Sci.*, **182**, 109278 (2021).
- M. Radovanović, M. P. Mihajlović, Ž. Tasić, A. Simonović, and M. Antonijević, *J. Mol. Liq.*, **342**, 116939 (2021).